CHAPTER 7. FIELD TESTS OF THE PERFORMANCE OF NEURAL NETWORK NOISE PREDICTION FILTERS

7.1 Application of noise prediction filters to AEM (SALTMAP) data

Three-component SALTMAP data were acquired at Lawlers, Western Australia, in February 1994 from 08:38:16 to 17:08:28. These measurements were carried out without any sferics rejection algorithm. Figures 7.1 and 7.2 show the X- and Z-component profiles, respectively, of a three-minute portion (in the afternoon from 16:01:41 to 16:04:57) of the SALTMAP data. These X- and Z-component profiles were obtained with 200 stacks. The vertical axis represents the amplitude in μV/A (transmitter current is ±70 A) and the horizontal axis is the flight line distance in metre. The X- and Z-component profiles at a flight line distance of 0 to 3100 m are considered to be the EM responses from a highly resistive area compared to the responses at a flight line distance of 3100 to 9100 m. As shown in Figures 7.1 and 7.2, the X-component AEM responses are about two times smaller than the Z component responses. However, the horizontal component of sferics noise is generally ten times larger than the vertical component (see Section 4.5 of Chapter 4). Therefore, it is considered that the X-component AEM response would be affected by relatively higher sferics noise than the Z-component response. Sharp Spikes shown on the X-component SALTMAP profile are caused by GPS noise and these spikes are not seen on the Z-component profile.

Usually, an LNPF is applied before stacking, but non-stacked AEM data are not available to allow the application of an LNPF. The data that are available have been stacked over 200 responses and there appears to be little evidence of the presence of sferics in these data. Therefore, the question of whether sferics noise measured with ground-based systems could be detected in the stacked SALTMAP data was examined.

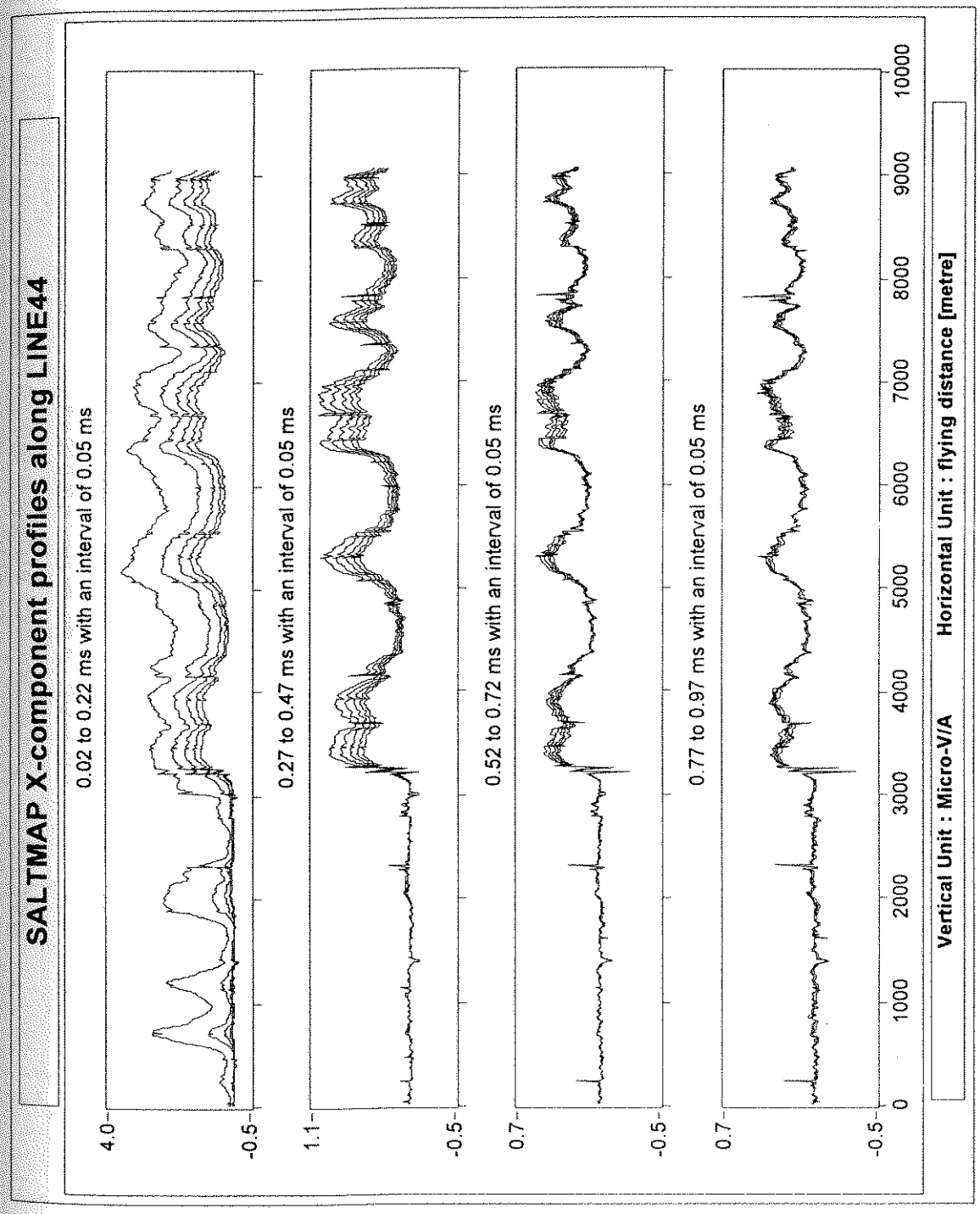

Figure 7.1 SALTMAP X-component profile obtained with 200 stacks.

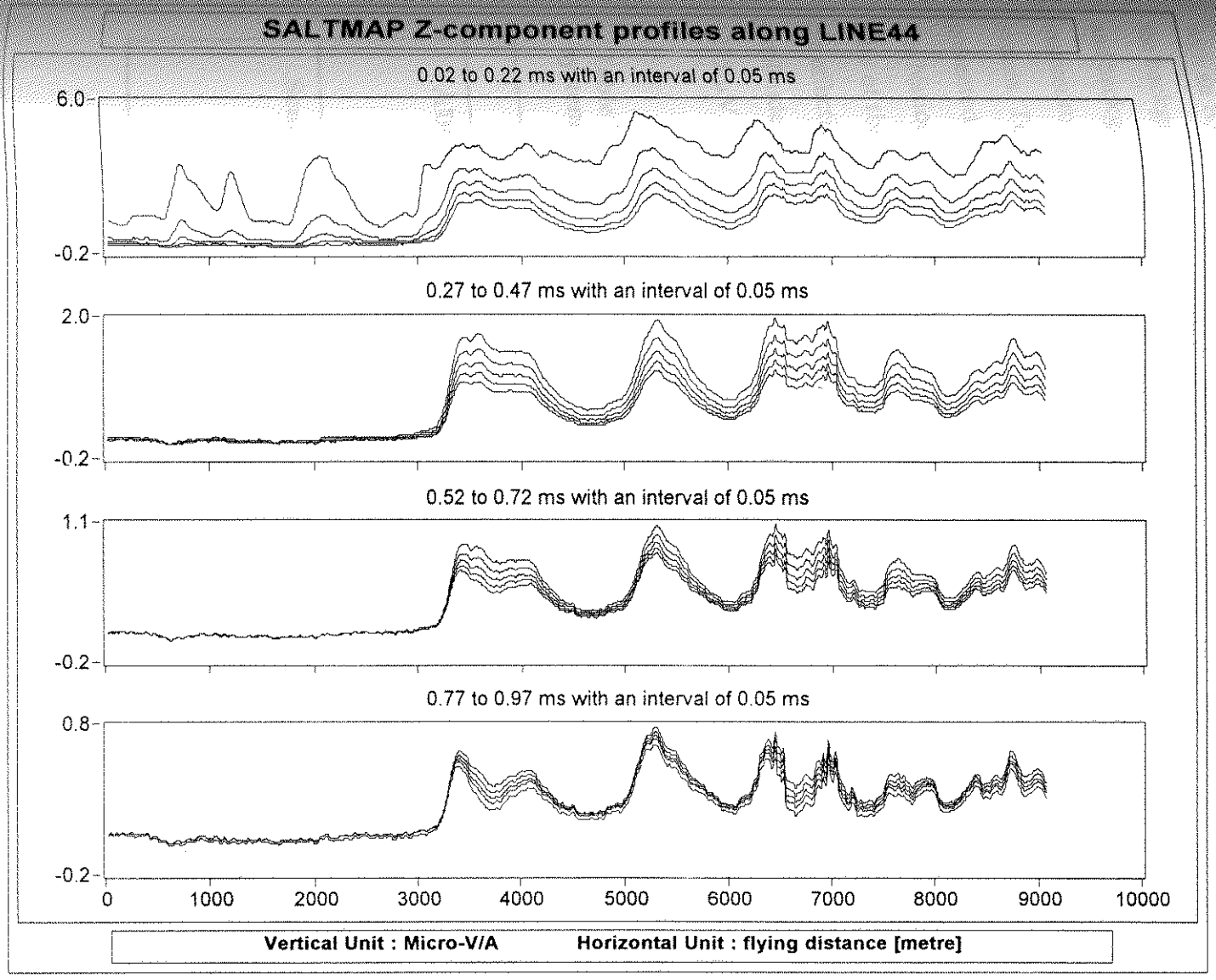

Figure 7.2 SALTMAP Z-component profile obtained with 200 stacks.

The maximum peak amplitude of the horizontal-component sferics measured with an RVR-3C at Ku-Ring-Gai National Park in February 1994 is about 1.7 V and the background noise level (mainly, VLF components) is about 50 mV. These sferics and background noise levels of 1.7 V and 50 mV, respectively, are taken to be the maximum and minimum amplitudes of detectable sferics noise by the SALTMAP system. To determine the range of sferics amplitudes expected on the SALTMAP data presented in Figure 7.1, the maximum and minimum amplitudes observed at Ku-Ring-Gai National Park are divided by the number of stacks (200), and multiplied by the ratio of the effective area of the SALTMAP horizontal-component coil (1500 m^2) to the effective area of the RVR-3C (10^4 m^2) (see Table 7.1). The expected peak amplitude range of sferics pulses in the X-component SALTMAP data is 37.5 to 1275 μV.

Table 7.1 Comparison of the SALTMAP with the computer-based noise system.

		SALTMAP	Noise System
ADC	ADC bit	16 bits	12 bits
	Input range	±0.5 V	±5.0 V
	Quantising level	15.26 μV	2.44 mV
Sensor	Sensor	Inductive coil	Inductive coil (RVR-3C)
	Passive area	50 m^2	50 m^2 (X comp.)
	Pre-Amp. gain	30	200
	Effective area	1,500 m^2	10,000 m^2

Assuming the EM signals at two successive stations are same, the residual voltage obtained from subtraction of two successive transient responses consists of

ADC noise and sferics noise only. Figure 7.3 shows the X-component residual time series in units of Volts between two successive transients at flight line distances of 4490 and 4500 m shown in Figure 7.1. This residual time series was obtained from the X-component SALTMAP data shown in Figure 7.1 by multiplying the responses in unit of μV/A by the SALTMAP transmitter current (i.e., 140 A). The residual time series still shows residual EM responses at early times. Half the peak-to-peak voltage of the residual time series at a delay time of around 0.6 ms is about 10 μV which is much smaller than the expected minimum amplitude of sferics (37.5 μV). Similar tests with other eight-minute SALTMAP data measured in the afternoon show that the residual time series between two successive transients is smaller than the expected minimum amplitude of sferics. Therefore, even though the SALTMAP three-component data were measured in the afternoon of summer season, it is considered that the measurements were made during a period of very low or no local sferics activity (Buselli and Sattel, 1995: Personal Communication).

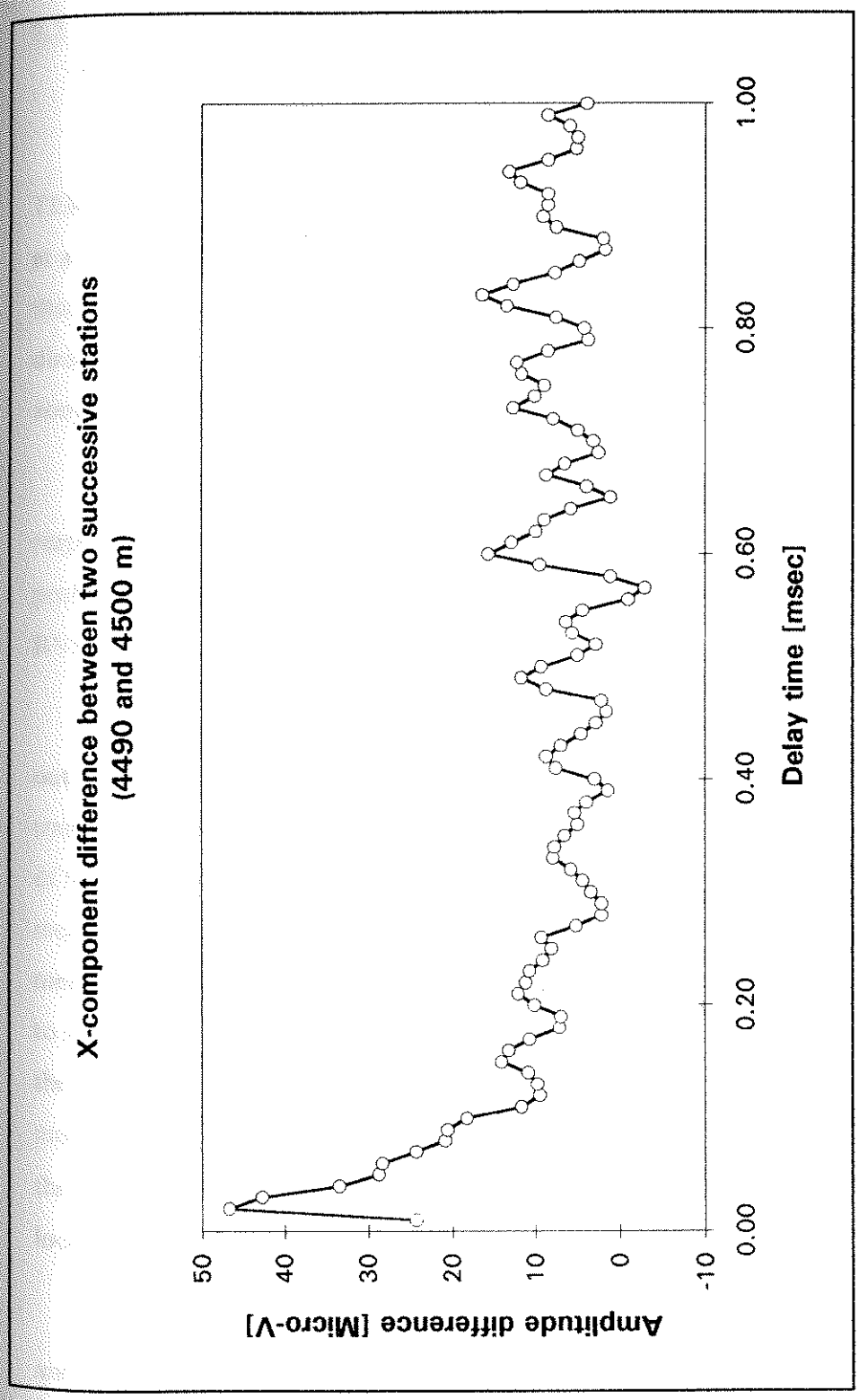

Figure 7.3 X-component residual time series obtained from subtraction of two successive transient responses.

7.2 Application of noise prediction filters to ground-based TEM data obtained in exploration conditions

In order to apply noise prediction filters (LNPF and RNPF) to ground-based TEM data obtained in exploration conditions, recordings of the TEM data were made at a mineral prospect near Parkes, NSW in August, 1995. Geologists have suggested that the mineralised zone is located around 10000N (Figure 7.4) and its strike and dip directions are east-west and south, respectively. The strike length of the mineralised zone is about 100 to 150 m and its depth extent is about 40 m (Figure 7.5).

For application of an LNPF, three orthogonal components of the TEM responses were measured with an in-loop geometry at a station interval of 50 m along profile 9900E (Figure 7.4). The transmitter loop size was 100 m×100 m and an RVR-3C was used as a sensor.

For application of an RNPF, the traverse with the in-loop geometry was carried out with a remote reference receiver 2 km north of the traverse. In addition, a fixed transmitter loop survey was carried out with the remote reference receiver 4 km north of the survey line. In both cases, the primary receiver along profile line 9900E measured the TEM signal and EM noise and, at the same time, the remote receiver measured solely the corresponding EM noise. GPS one-second time pulses were used to synchronise the three-component measurements at the two separated receivers. At the primary site, the TEM measurements with the fixed- and in-loop geometries were made with intervals of 25 and 50 m, respectively, along profile line 9900E. The size of the fixed-loop was 300×300 m and an RVR-3C was used as the sensor at both the local and remote site.

SIROTEM measurements were also made along line 9900E with both in-loop and fixed-loop geometries. The SIROTEM measurements were made with 25 windows

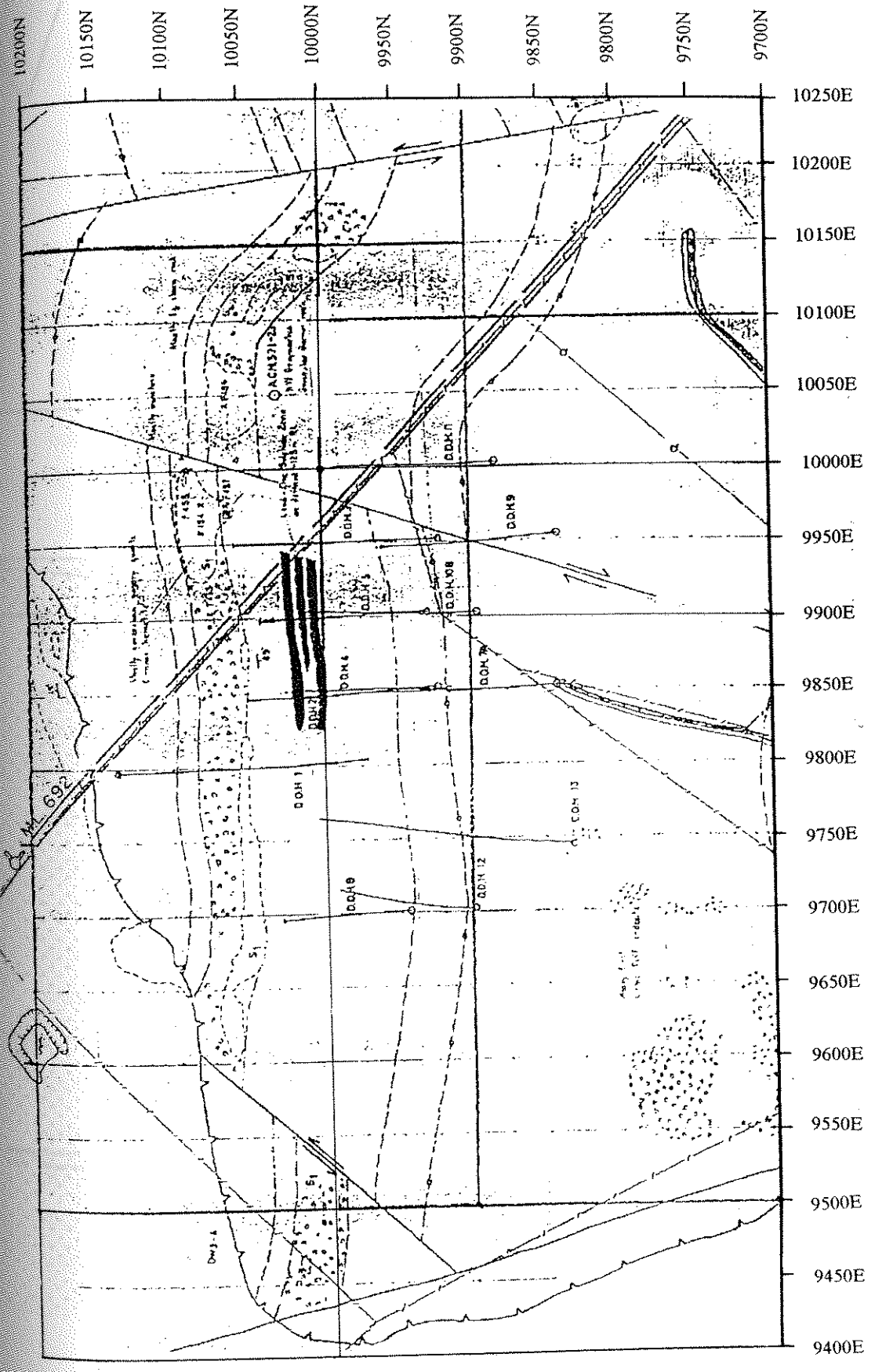

Figure 7.4 TEM survey map of a mineral prospect near Parkes, NSW.

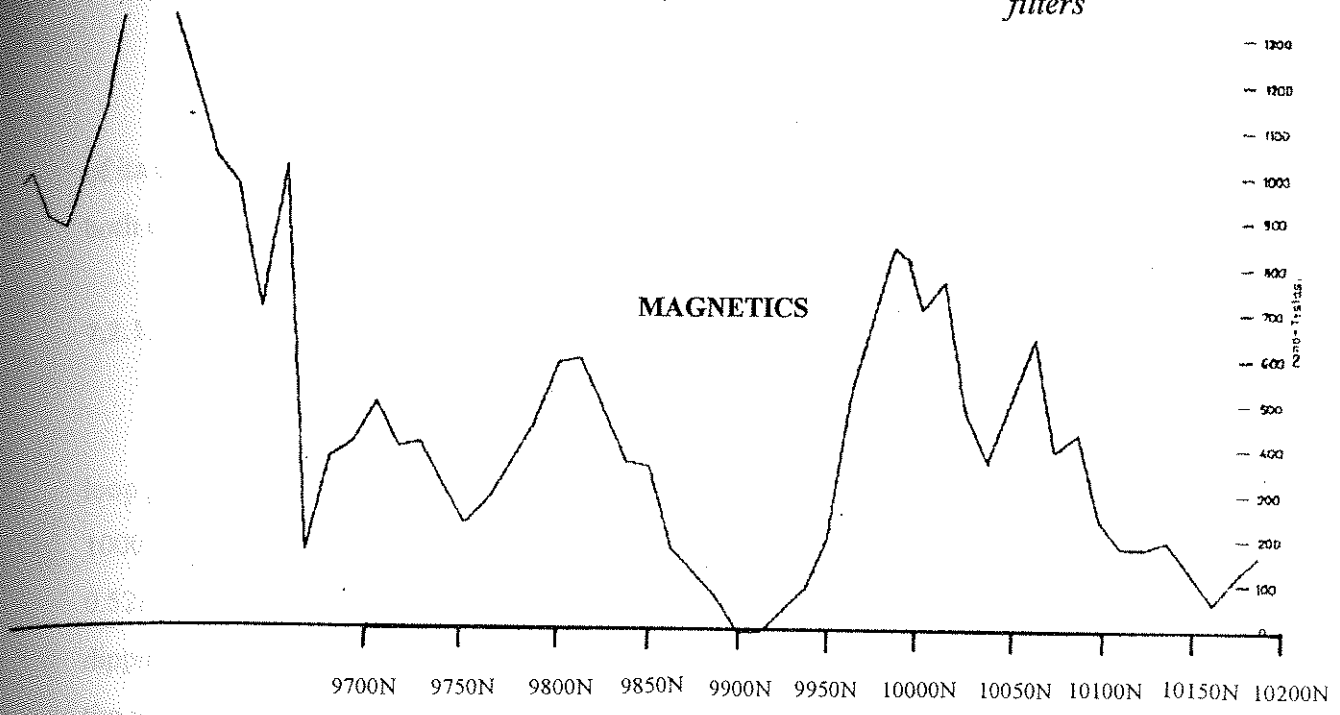

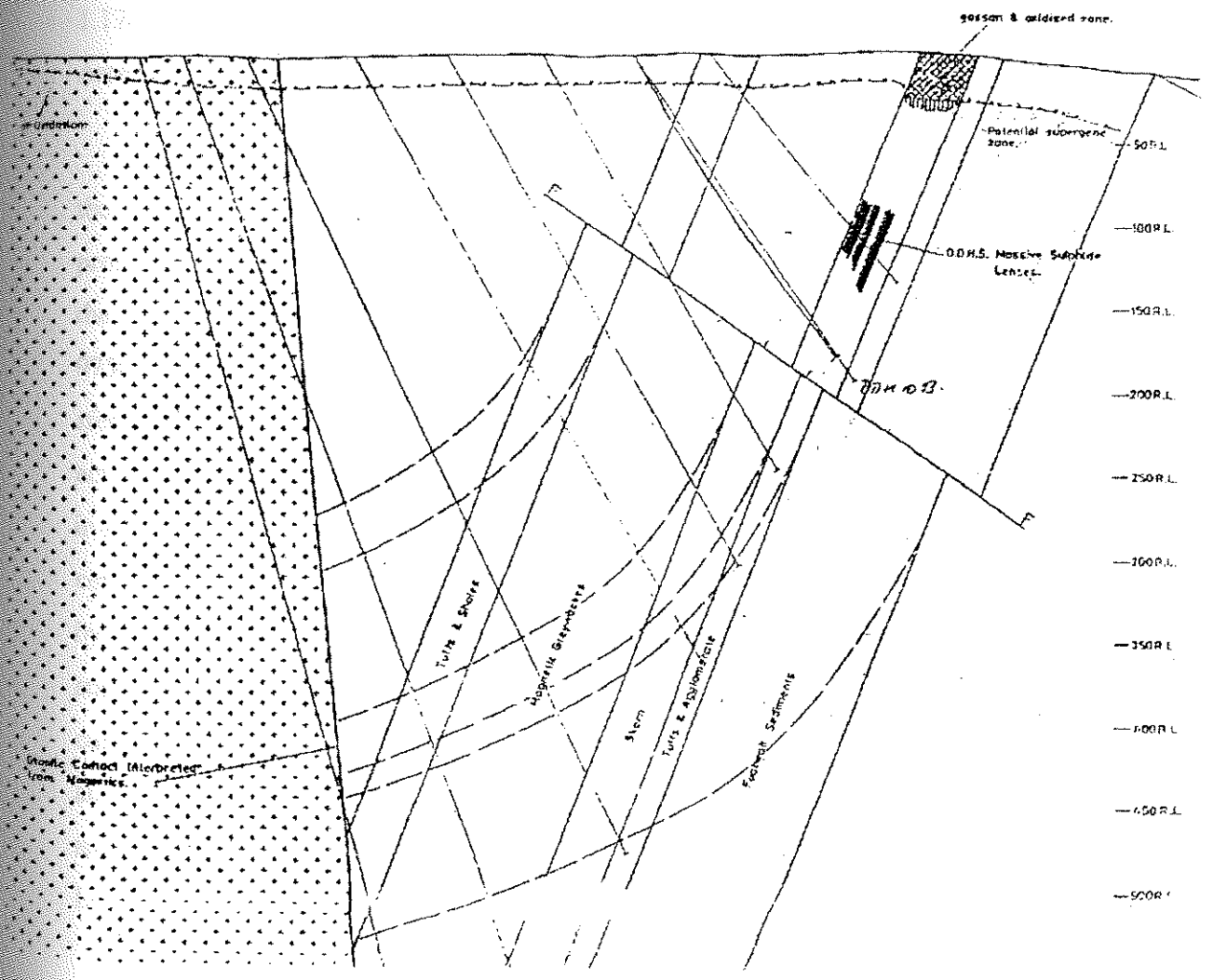

Figure 7.5 Vertical section of mineral deposit along profile 9900E shown in Figure 7.4.

of its composite delay time range, and therefore the transmitter on- and off-times were both of 20 ms duration.

7.2.1 Local noise prediction filter

Figure 7.6 shows the TEM response profile of a SIROTEM survey with an in-loop geometry along 9900E line. The TEM profile was obtained with 2 repeat runs of 1000 stacks each. The small peaks at stations 9950N and 10150N at delay times of 0.528 to 0.778 ms suggest that the conducting body causing the anomalous response is dipping steeply to the north, i.e., in a direction opposite to the dip of the geology and the mineralised zone shown in Figure 7.5. The TEM responses at delay times after 1.178 ms have negative values considered to be caused by an IP effect (as described by Asten and Price, 1985; Smith and West, 1988).

Figure 7.7 shows the in-loop geometry TEM response profile measured with the computer-based noise system (see Section 2.1.1 of Chapter 2). Even though this profile was obtained with one bipolar stack and without an LNPF, it is very similar to the corresponding SIROTEM profile plotted in Figure 7.6. At most stations (except 9750, 9950, and 10000N), the TEM response was not affected by sferics noise. The sferics count rate was 6 pulses per sec during measurements. Therefore, the sferics activity at Parkes in winter was very low compared to the sferics count rate in Darwin in summer (Table 2.1). However, the TEM response at station 9950N in windows centred at delay times of 0.474, 0.572, and 0.724 ms was affected by sferics as shown by the TEM decay curve at station 9950N plotted in Figure 7.8. The response at station 10000N at a delay time of 0.924 ms was also affected by sferics (see decay curve in Figure 7.9). The Z-component TEM profiles obtained after applying an LNPF are shown in Figure 7.10. The LNPF achieves very effective performance at both 9950 and 10000N stations for reducing sferics noise. For example, at 10000N station, the LNPF improves the S/N ratio by a factor of 5.3 at delay times of 0.85 to 1.35 ms.

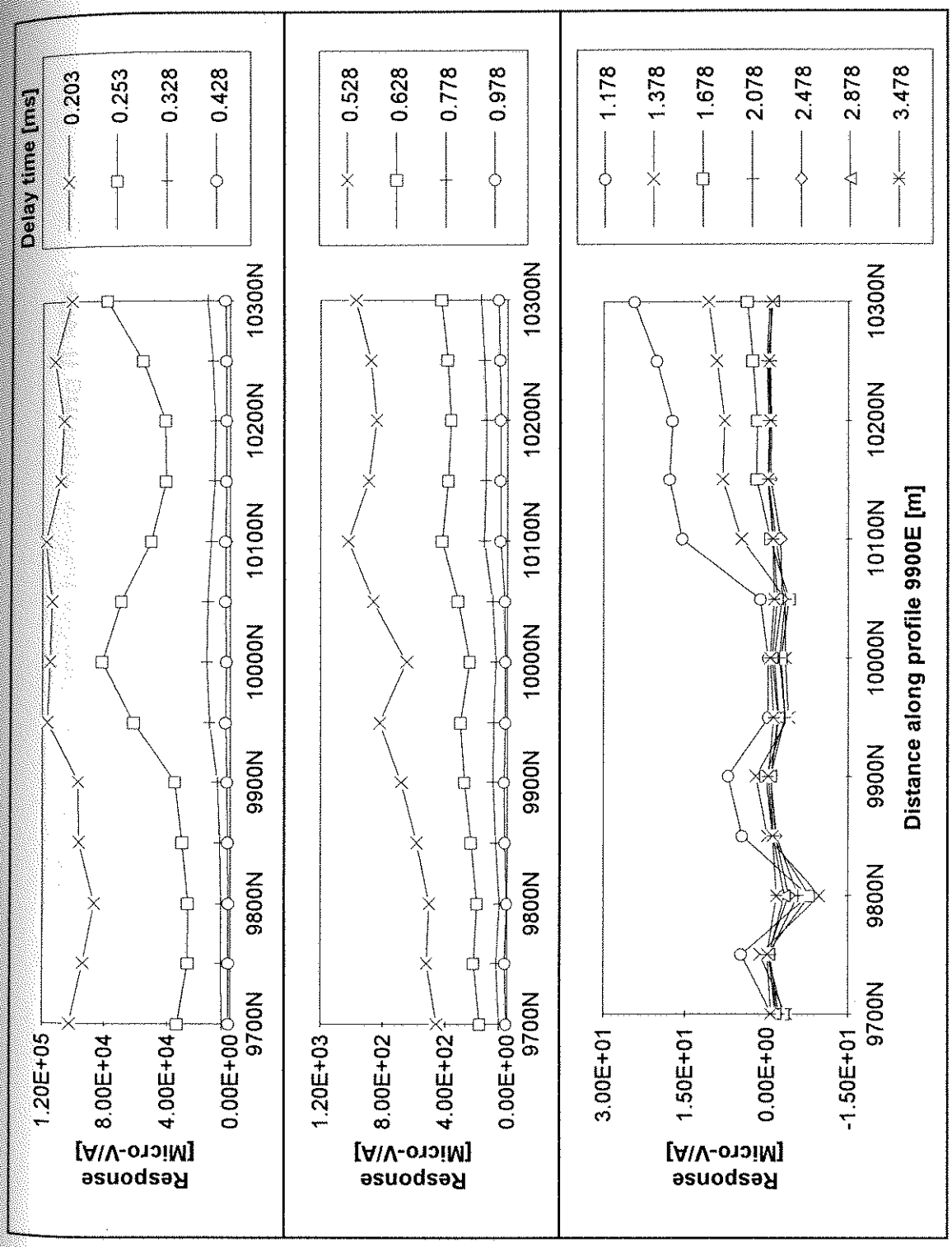

Figure 7.6 TEM response profile of a SIROTEM survey with an in-loop geometry along 9900E line.

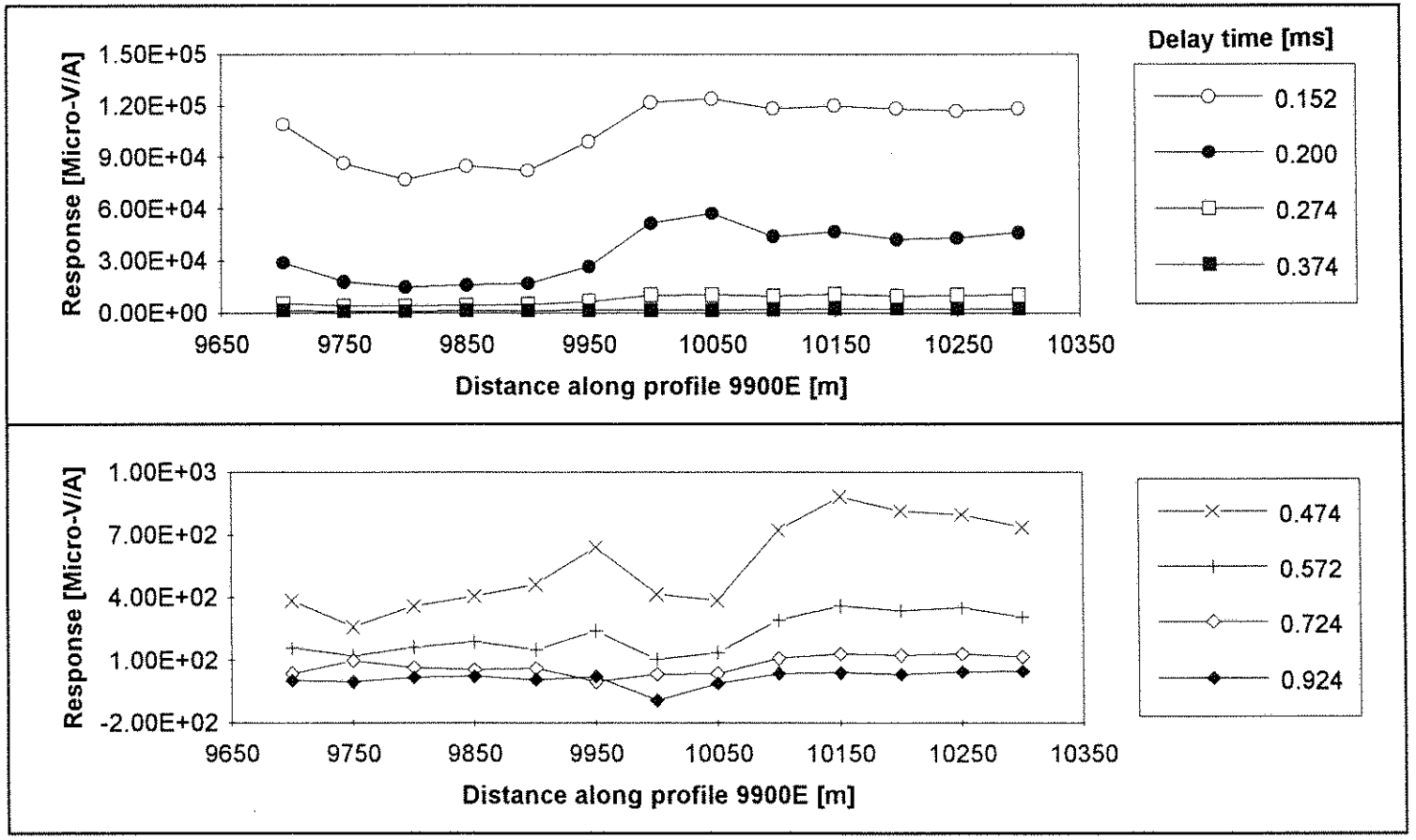

Figure 7.7 In-loop geometry TEM response profile obtained without applying an LNPF. These measurements were recorded with the computer based noise system.

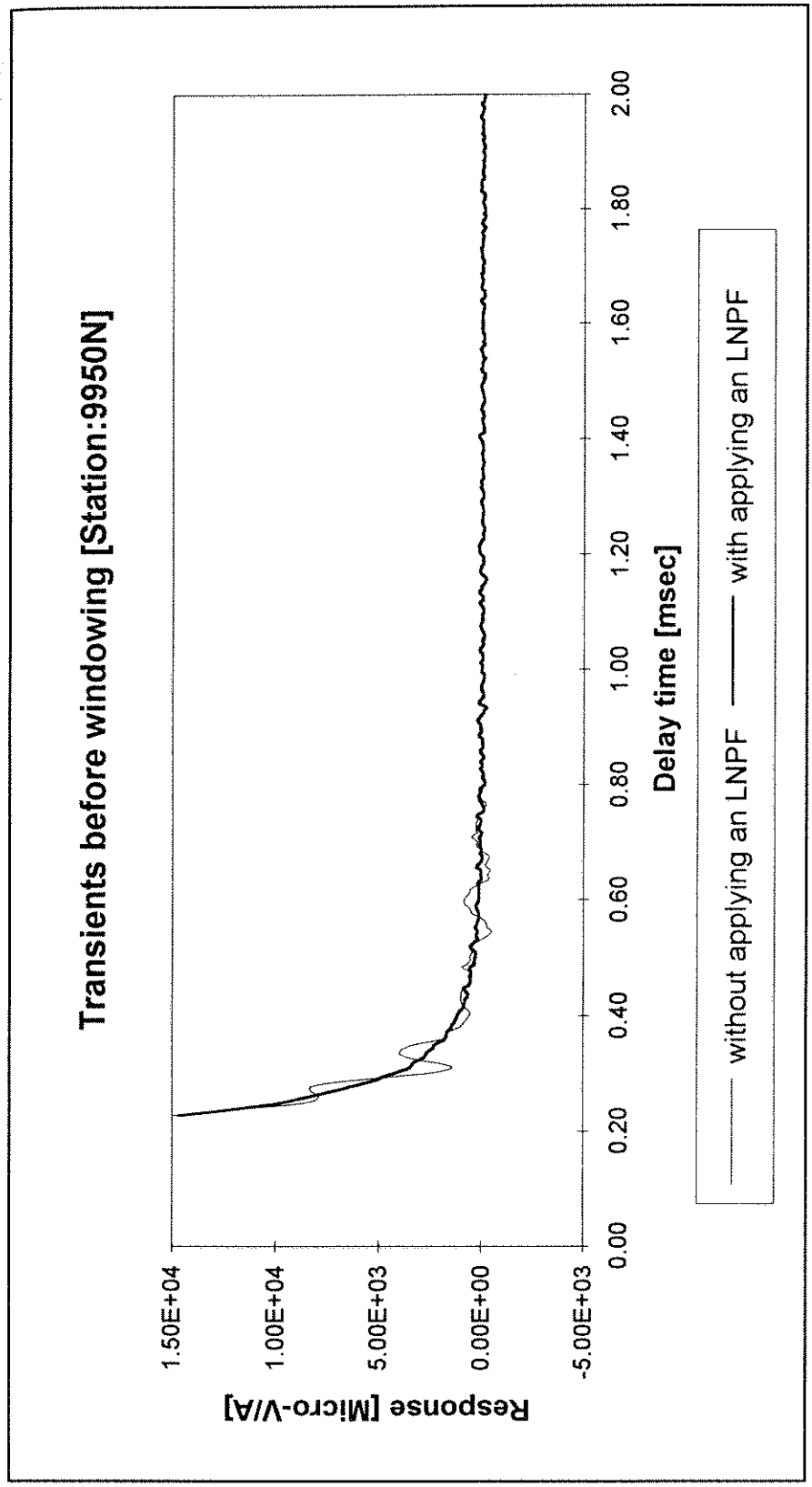

Figure 7.8 Transients with and without applying an LNPF at station 9950N.

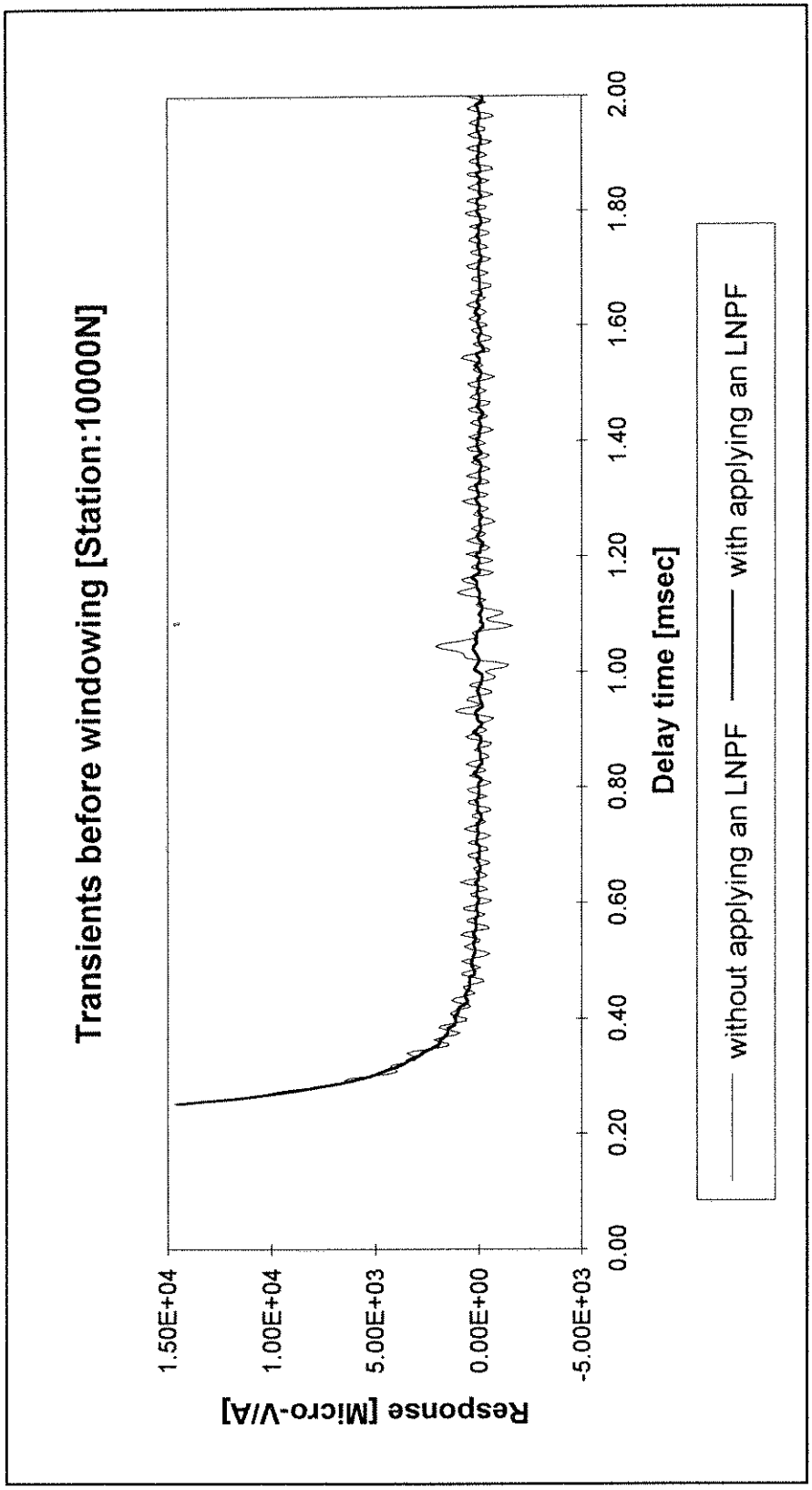

Figure 7.9 Transients with and without applying an LNPF at station 10000N.

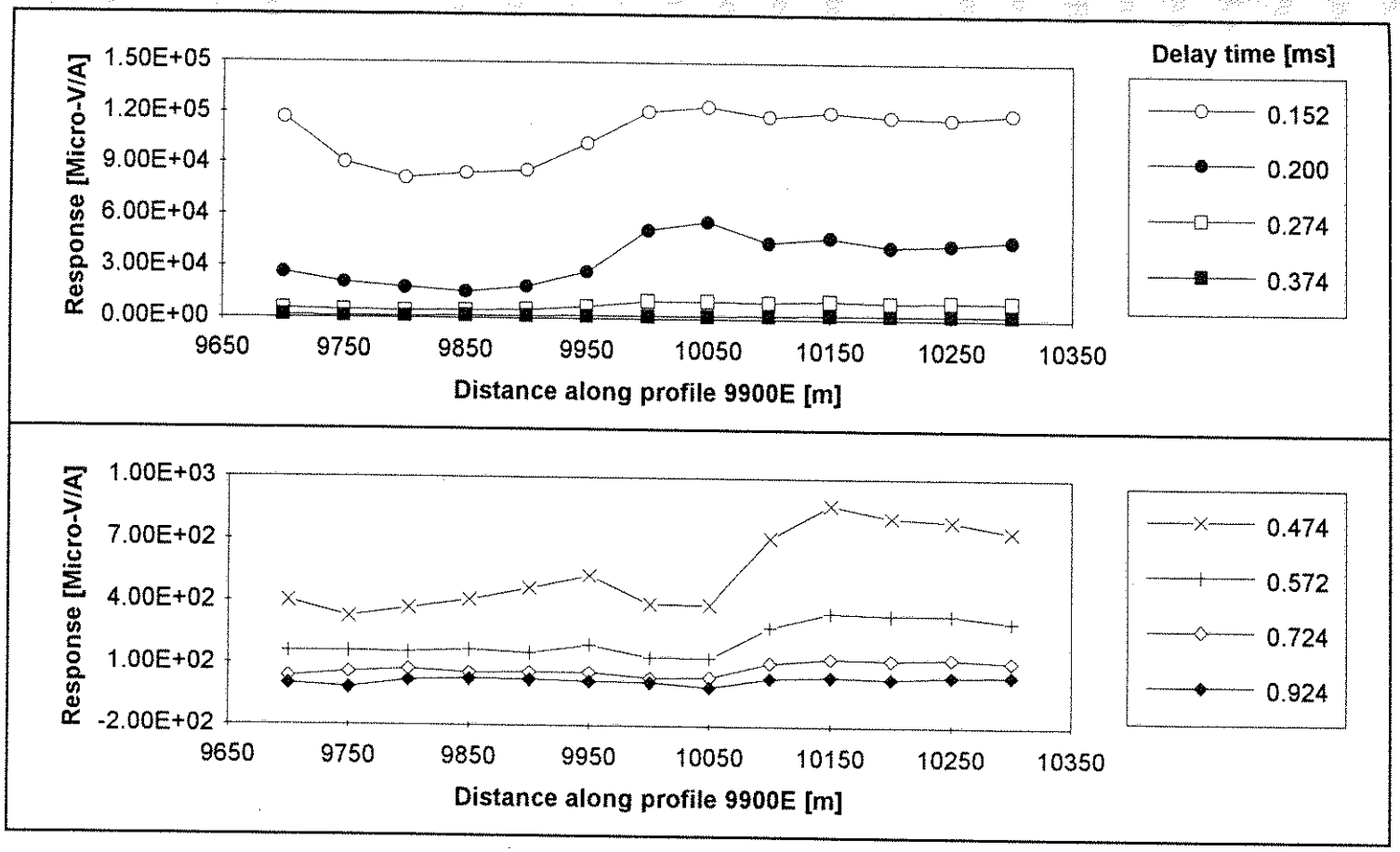

Figure 7.10 In-loop geometry TEM response profile obtained by applying an LNPF to the TEM response shown in Figure 7.7.

The assumption used in applying an LNPF to the TEM response measured over the horizontally layered earth with an in-loop geometry is that the horizontal component measures solely noise, whereas the vertical component measures both the TEM signal and correlated noise. However, when lateral changes in conductivity are present, a bias error will results when an LNPF is employed, since some of the TEM signal is present in the horizontal component. Spies (1988) has pointed out that this bias error is comparatively small and does not adversely affect interpretation of the in-loop TEM data. For a large TEM signal in the horizontal component, a first-order difference method (described in Section 7.2.2.1) to remove the TEM signal from the horizontal component can be applied before applying an LNPF.

Since the sferics activity at Parkes was low, the performance of the LNPF was evaluated by adding sferics measured in Darwin in December 1994 to the response recorded at Parkes. To simulate a noise-free transient, an exponential function was fitted to the in-loop TEM response at station 9950N. Three-component Darwin noise data added to this noise-free response was sampled at 250 kHz (i.e., a sample interval of 0.004 ms) for 5 sec. The count rate of sferics pulses in this time series was 76 sferics pulses/sec. This count rate was obtained using a threshold of 20% larger than any variations in background EM noise level and a deadtime of 1 ms after the occurrence of any sferics pulse.

In order to simulate noise obtained with SIROTEM windowing, two 20 ms blocks (transmitter off-time) of EM noise data separated by an interval of 20 ms (transmitter on-time) were chosen. A single bipolar stack was obtained by subtracting corresponding 4 μs samples of the second block from those of the first block and dividing the difference by 2. The time series indicated by the dotted line in Figure 7.11 was obtained from averaging 50 bipolar stacks without applying an LNPF. The time series obtained by applying an LNPF to each bipolar stack and then averaging 50 of these stacks is represented by the bold line plotted in Figure 7.11. A noise reduction

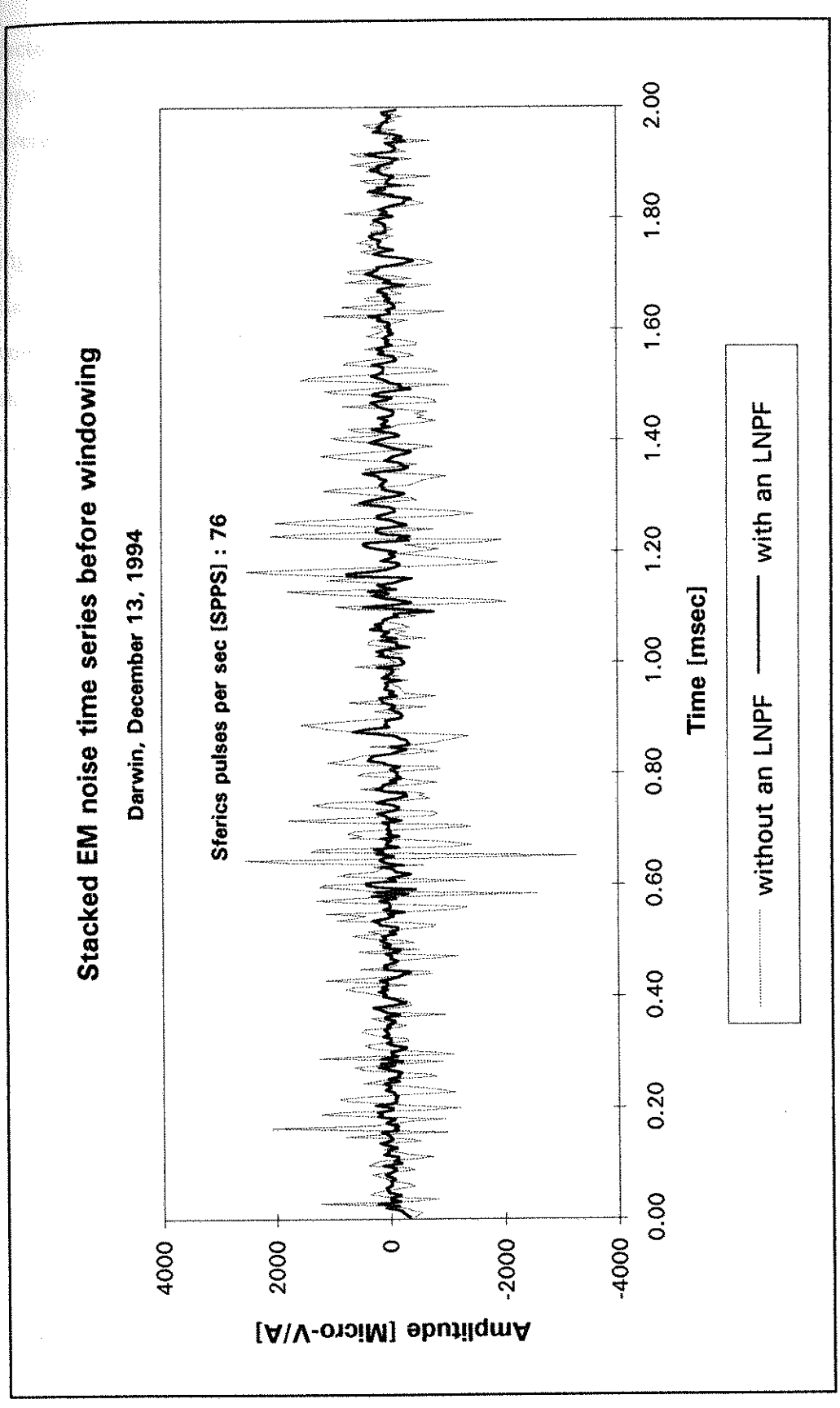

Figure 7.11 Time series obtained with and without applying an LNPF to each bipolar stack before averaging over 50 such stacks

factor of 3.4 was obtained from calculating the RMS of the average of fifty 20-ms bipolar stacks of the noise without use of the LNPF and dividing by the corresponding average obtained by stacking after applying the LNPF to each bipolar stack.

Figure 7.12 shows the noise obtained when the stacked noise samples of Figure 7.11 were windowed according to the SIROTEM composite time scheme. Results are shown for the use of an LNPF (heavy line) applied to each bipolar stack compared with the case of no LNPF (light line) applied to the stacks. Figure 7.13 shows results obtained when the windowed noise was added to the generated noise-free transient at station 9950N. The simple-stacked and filtered-stacked transients show that at late delay times (0.924 to 1.624 ms), the LNPF improves a S/N ratio by a factor of 4.1 compared to the simple stacking.

7.2.2 Remote noise prediction filter

7.2.2.1 Horizontal components

In applying an RNPF, any time shift between corresponding sferics pulses measured at the local and remote stations needs to be removed. In order to calculate the time shift between a local and remote time series when TEM signal is present in the local receiver, a first-order difference method, which requires subtraction between two successive samples of a given transient response, was applied to remove the TEM signal. Figure 7.14 shows an example when the first-order difference method was applied to the time series recorded at 10050N and to the corresponding time series measured simultaneously at the remote reference station. As shown by comparing the two time series before and after applying the first-order difference at the local station, the TEM signal is clearly removed.

To demonstrate how the first-order difference method works, the cross-phase spectrum between the local sferics pulse measured at a delay time of 2 ms

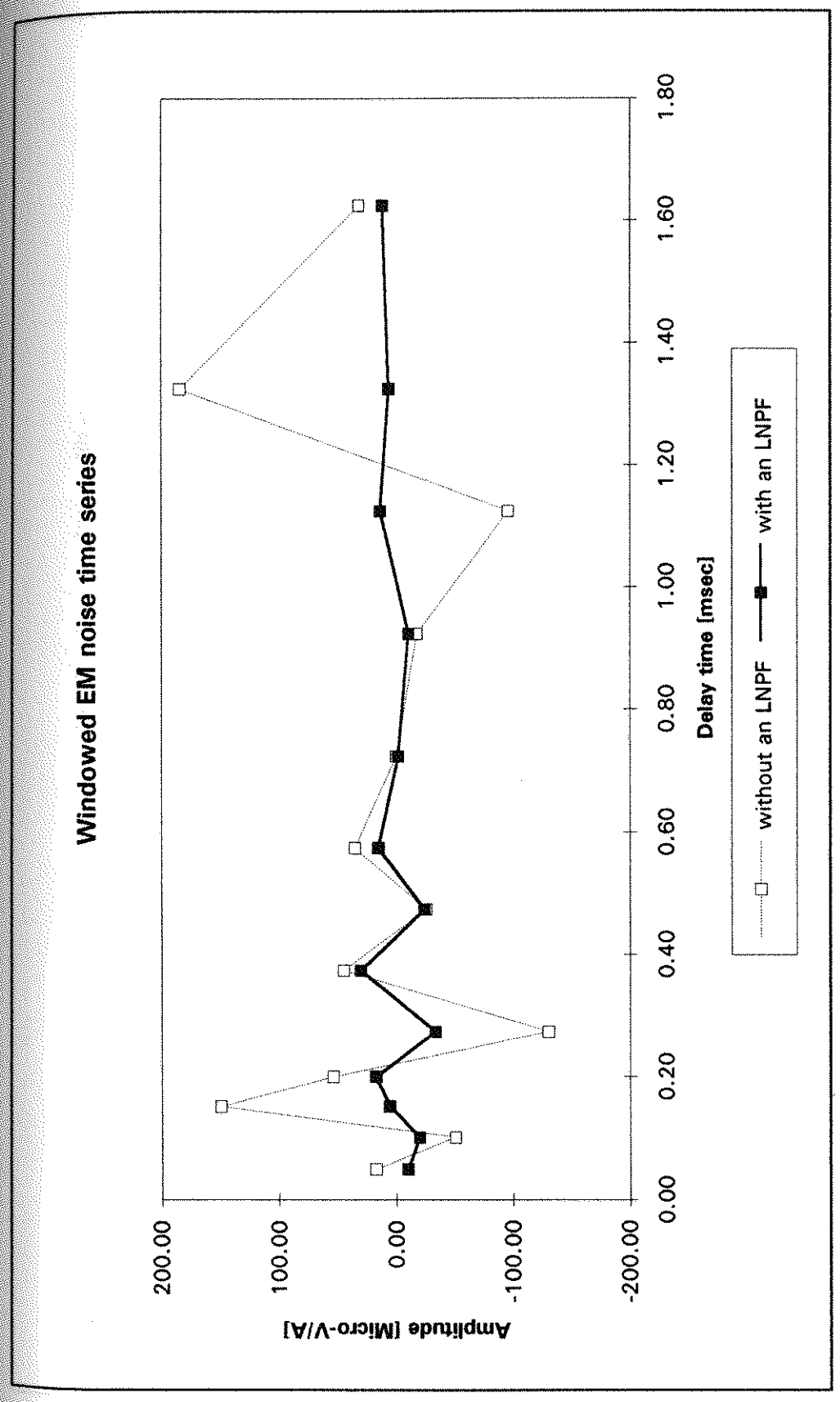

Figure 7.12 Two windowed noise time series when the 50-bipolar stacked time series shown in Figure 7.11 were windowed according to the SIROTEM composite time scheme.

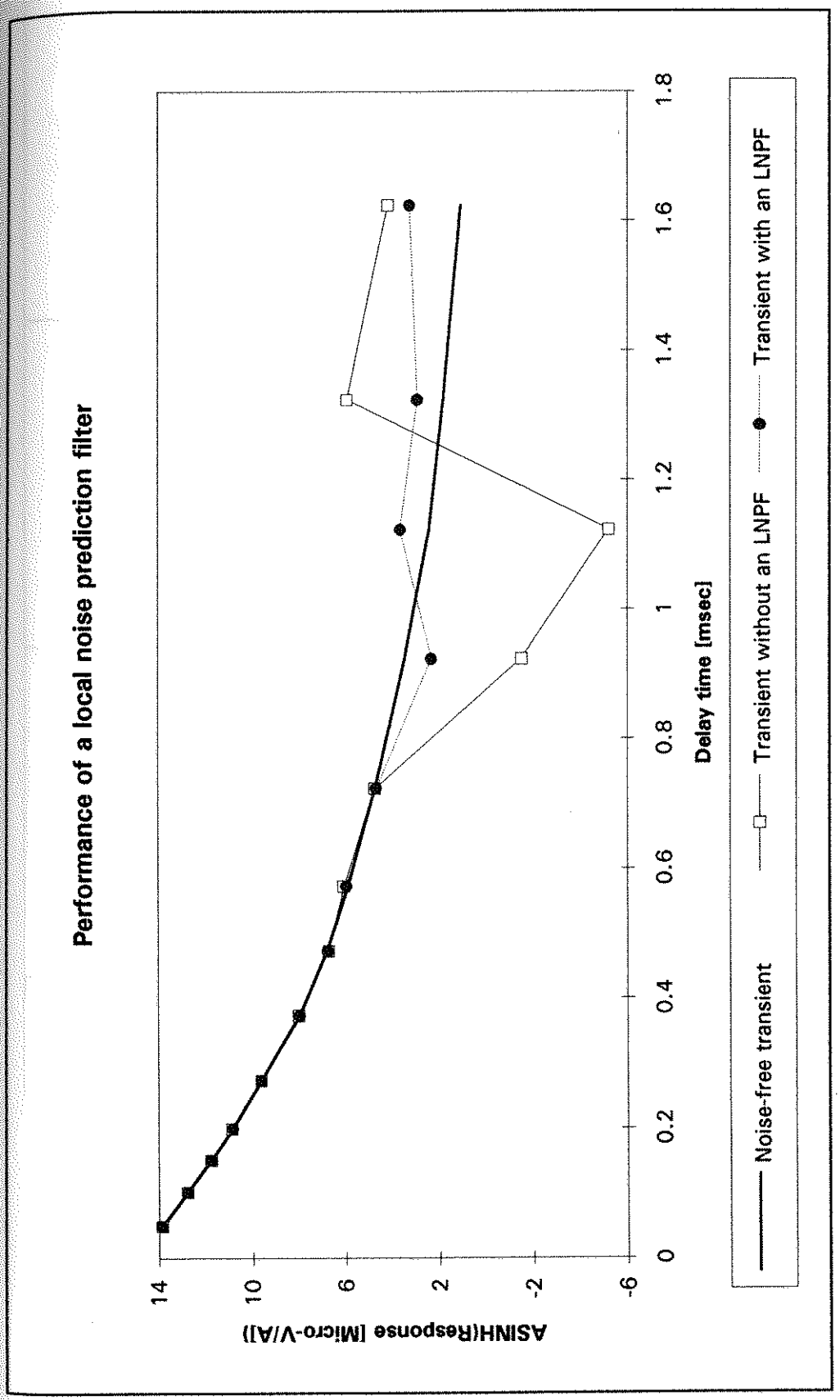

Figure 7.13 Example of results when the windowed noise shown in Figure 7.12 was added to the generated noise-free transient at station 9900N.

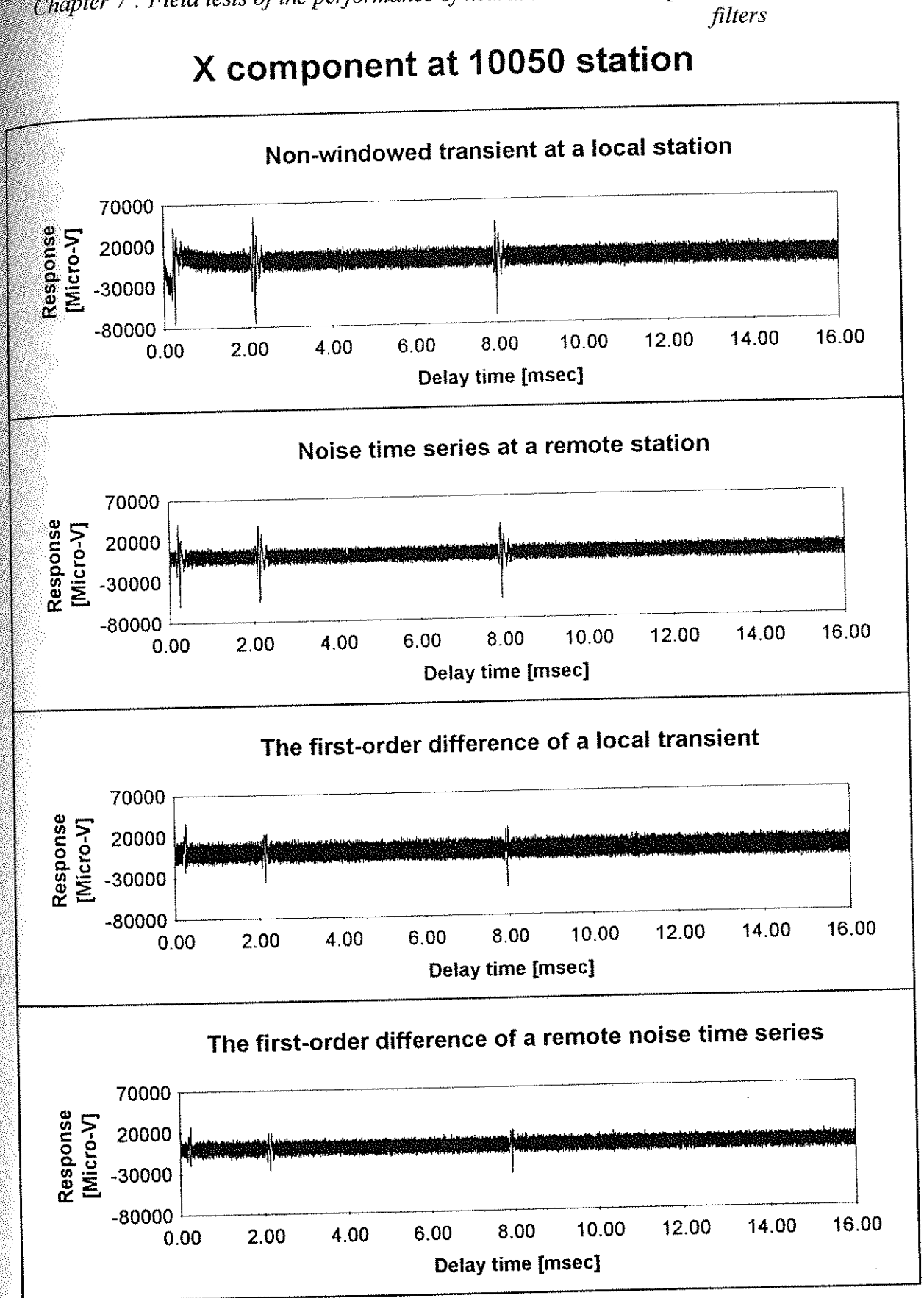

Figure 7.14 Example of the application of the first-order difference method to the non-windowed fixed-loop TEM responses recorded at station 10050N and to the corresponding time series measured simultaneously at the remote reference station.

(Figure 7.14) and the corresponding remote sferics pulse is presented at the top diagram of Figure 7.15. The plot at the bottom of Figure 7.15 shows the cross-phase spectrum obtained after the first-order difference of successive samples has been applied to both time series. The time shift between the local and remote sferics pulses is determined from the slope of the cross-phase spectrum in a given frequency range (see Appendix A2.6). Using either of the plots in Figure 7.15, a value of 3.7 μs in a frequency range of 5 to 35 kHz (where power is contributed by sferics) is obtained for the time shift between the two sferics pulses. Thus, application of the first-order difference method to remove the local transient response does not affect the determination of the time shift between given local and remote sferics pulses.

Figure 7.16 shows the X-component TEM profiles of single bipolar stacked TEM responses obtained with the fixed-loop geometry along profile 9900E. These profiles were obtained before applying an RNPF. The TEM responses at stations 9950, 10000, 10050, and 10125N were affected by sferics noise. For example, the response at station 10050N at a delay time of 0.2 ms can be well explained by the raw transient shown in Figure 7.17. This non-windowed transient at the local receiver was obtained with a single bipolar stack. Three sferics pulses shown on this local transient are strongly correlated with sferics pulses shown in noise time series at the remote station. The two filtered transients obtained from simple subtraction of the remote response from the local response and from application of an RNPF show that the RNPF suppresses sferics pulses at the local receiver with an *NRF* of 4.0, while the transient from simple subtraction still shows the residual sferics noise (with an *NRF* value of 2.6).

Figure 7.18 shows the profiles after applying an RNPF. At most stations affected by sferics noise (e.g., 9950, 10000, 10050, and 10125N stations), the profiles obtained from an RNPF are smooth, and the spikes shown in Figure 7.16 (e.g., late time responses at 9950N station) have been reduced. At stations 10225, 10250, and 10275N, noisy TEM responses at delay times of 0.1 to 0.2 ms were affected by some

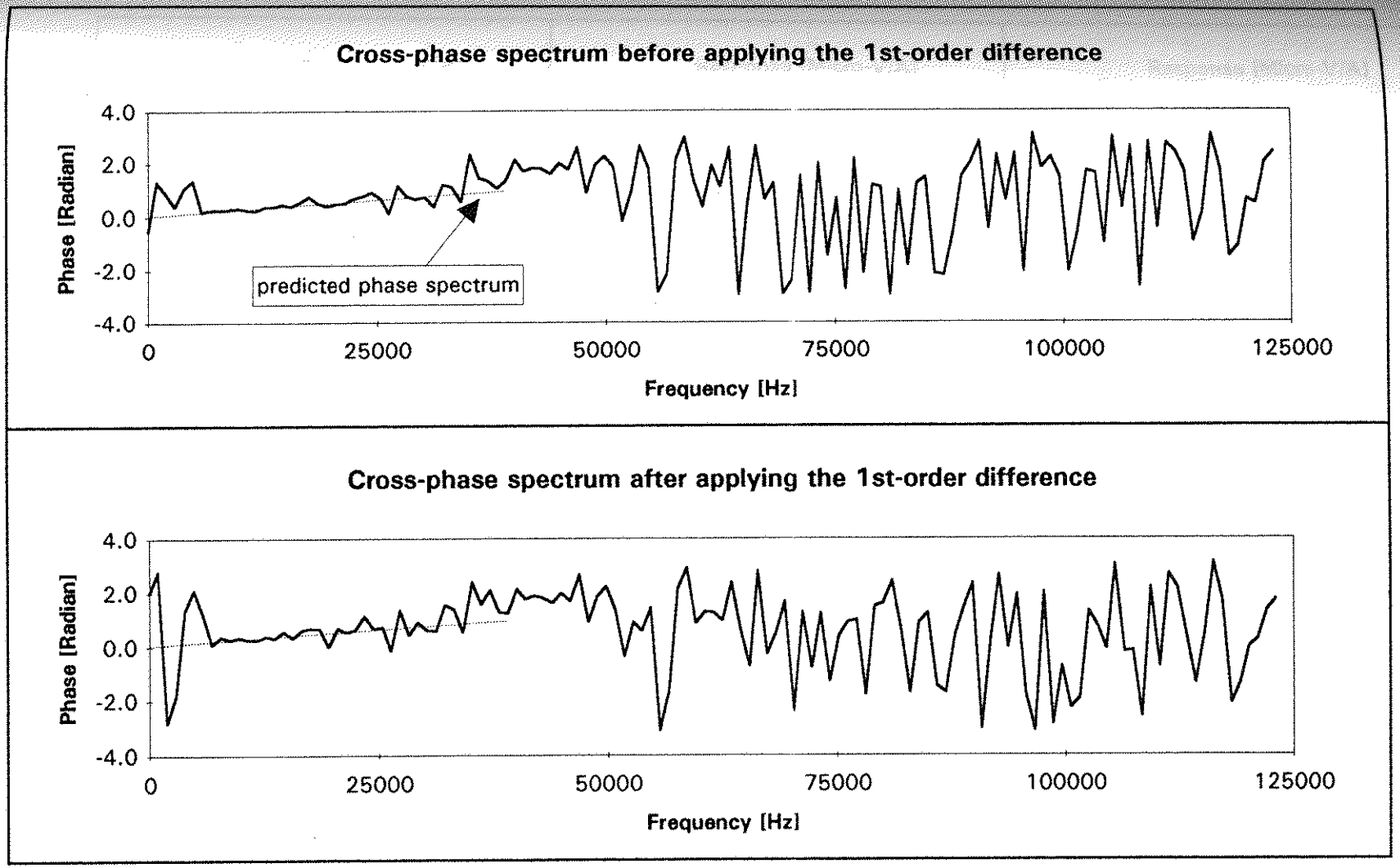

Figure 7.15 Cross-phase spectra obtained before and after applying the first-order difference method to the local and remote time series shown in Figure 7.14.

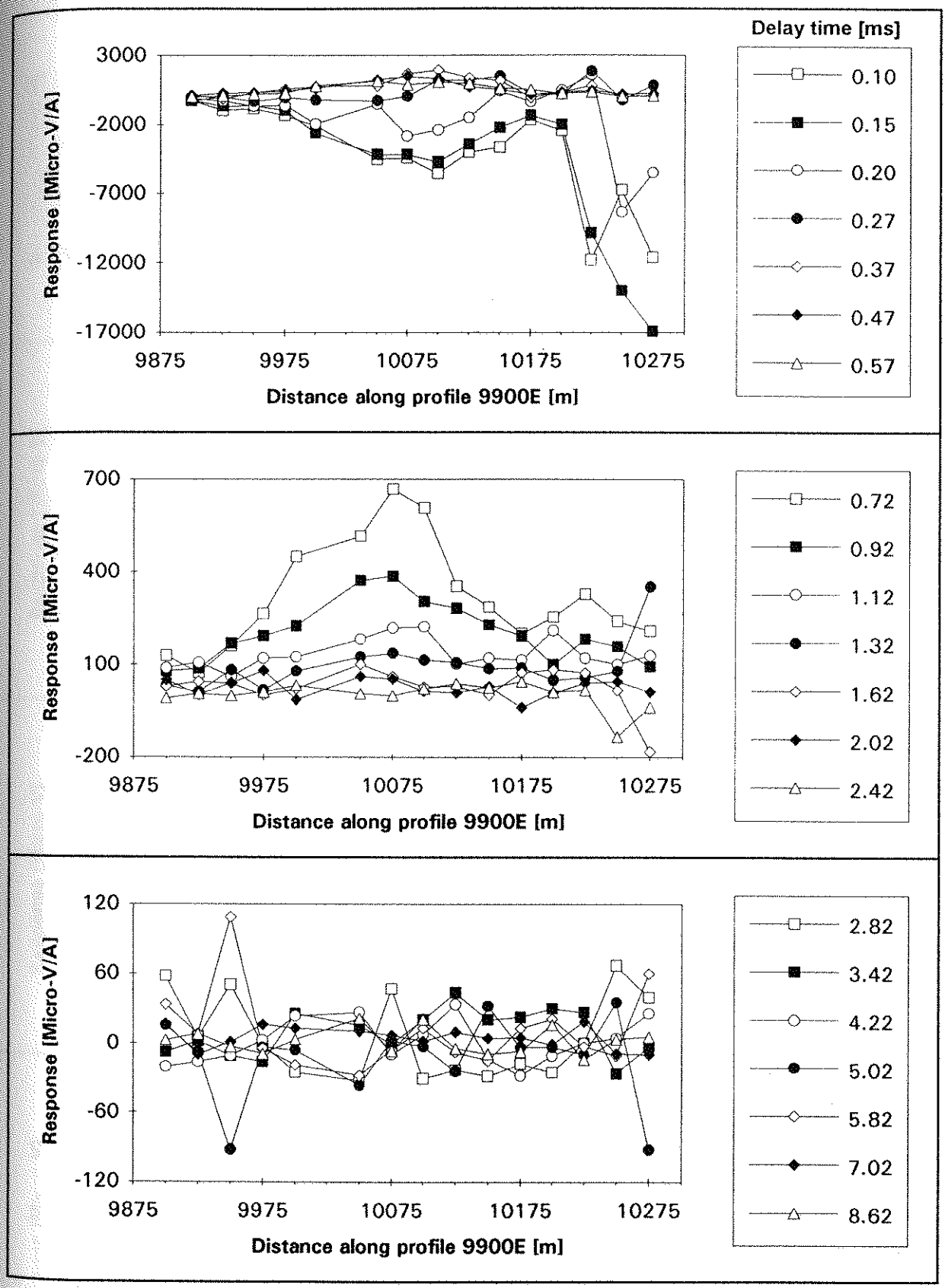

Figure 7.16 Fixed-loop geometry X-component TEM response profile along profile 9900E obtained without applying an RNPF. These measurements were recorded with the computer-based noise system.

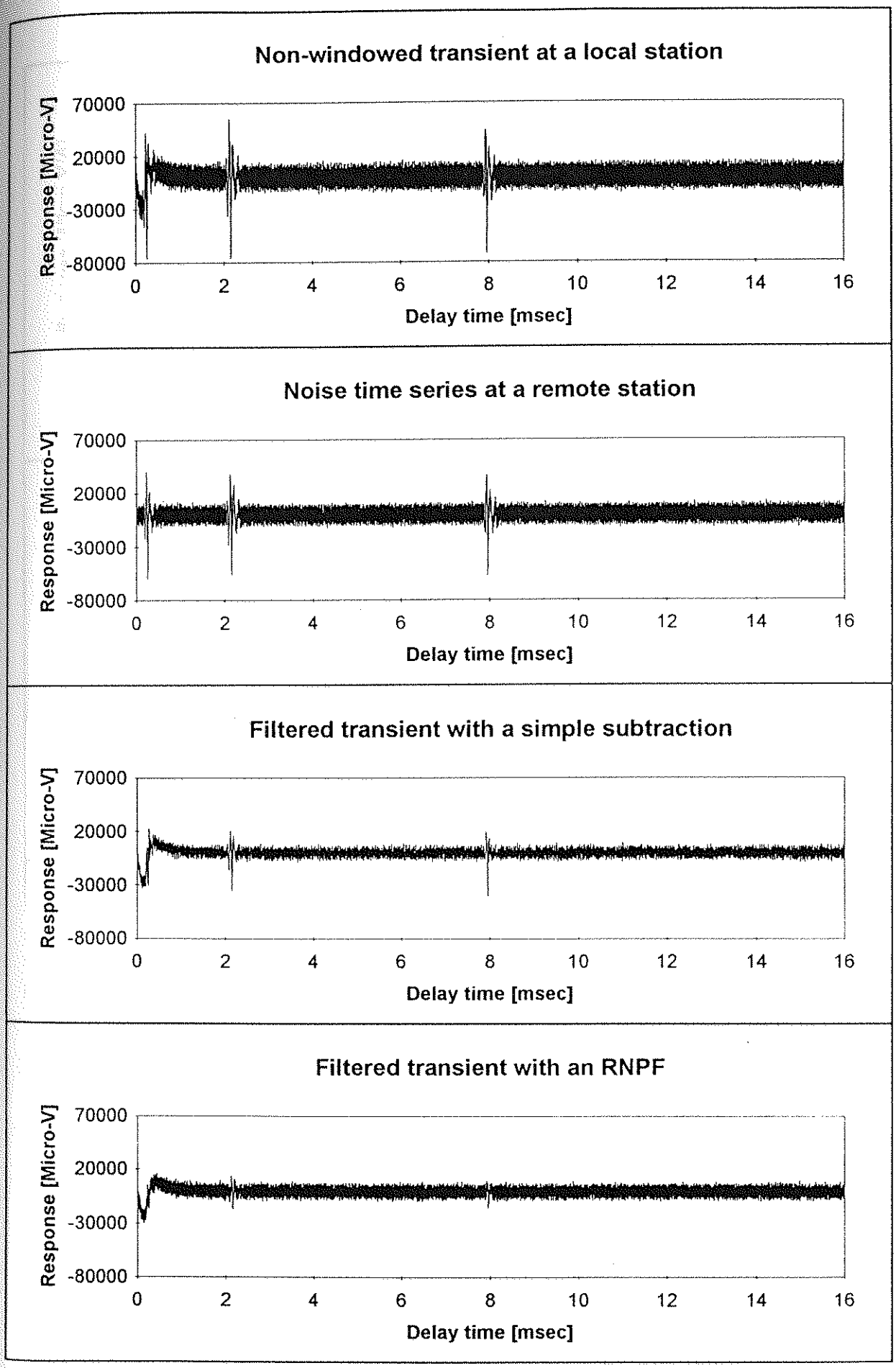

Figure 7.17 Comparison when an RNPF and simple subtraction were applied to the X-component time series measured simultaneously at station 10050N and the remote station.

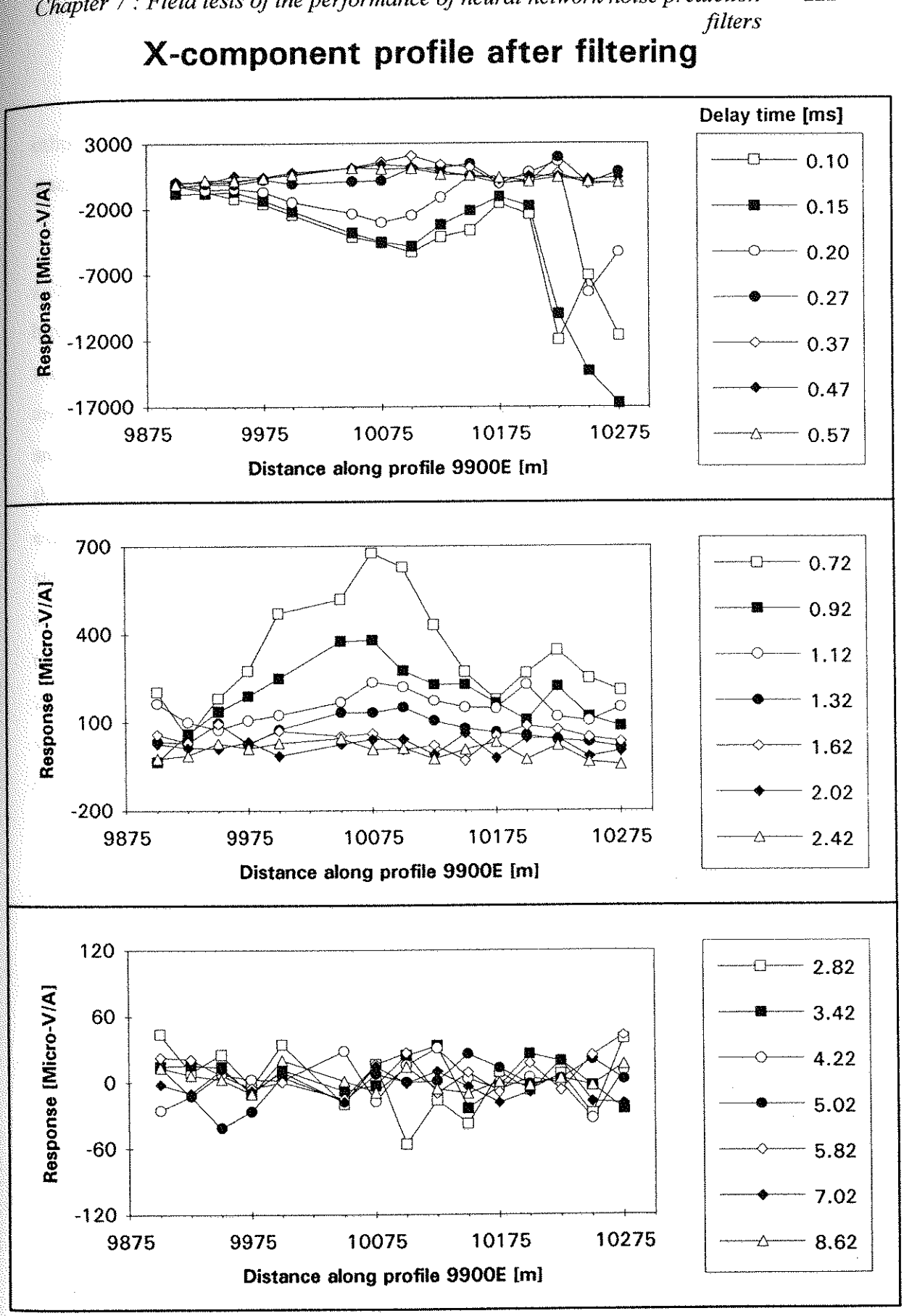

Figure 7.18 Fixed-loop geometry X-component TEM response profile along profile 9900E obtained by applying an RNPF. These measurements were recorded with the computer-based noise system.

other unknown noise source rather than sferics. Similar noise was observed in 1000 stacked SIROTEM data which were measured at a different time (Figure 7.19).

Figures 7.20 and 7.21 show the Y-component profiles before and after applying an RNPF, respectively. At each station, responses have been averaged over a single bipolar stack only. These Y-component responses were measured simultaneously with the X-component responses shown in Figure 7.14. Since the Y-component responses are larger than the X-component responses, the Y-component profiles appear to be smoother than the X component profiles. However, at stations 10000N and 10050N, the responses at delay times of 2.02 and 2.42 ms clearly show sferics noise. As an example of the performance of an RNPF and simple subtraction with the Y-component sferics at station 10050N, Figure 7.22 shows that the RNPF reduces significantly three sferics pulses, while the filtered transient obtained from simple subtraction still shows the residual sferics pulses even greater than background noise. *NRF* values of 4.8 and 2.4 were obtained with the RNPF and simple subtraction, respectively, when the *NRF* value was calculated on the third sferics pulse (at delay time of about 8 ms) shown in the top diagram of Figure 7.22.

In order to evaluate the performance of an RNPF with high sferics activity data, local and remote sferics data measured with 1 km separation in Darwin in December 1994 were used. The sferics count rate of the X component is 82 pulses per sec, which is at least 13 times higher than the sferics activity of Parkes data. The two non-windowed noise time series with and without an RNPF shown at the top of Figure 7.23 were obtained with 50 stacks as mentioned in the previous section. An *NRF* value of 4.7 was obtained with the RNPF, while simple subtraction suppressed noise by a factor of 3.4 (the noise time series obtained with simple subtraction is not plotted in Figure 7.23).

To illustrate reduction of high sferics noise on a typical TEM response measured at Parkes, a noise-free transient response was derived from a fit to the

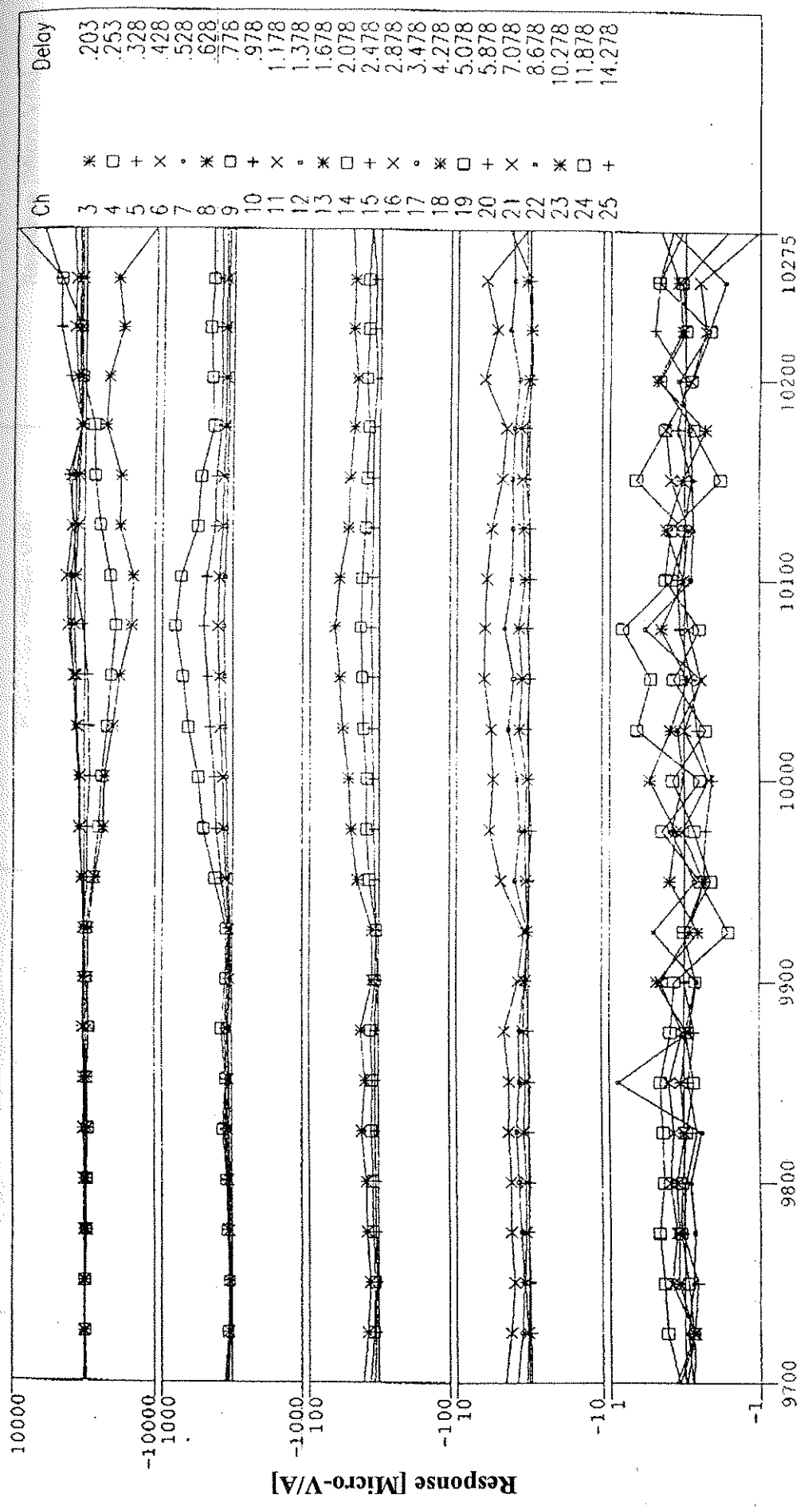

Figure 7.19 X-component TEM response profile of a SIROTEM survey obtained with a fixed-loop geometry along 9900E line.

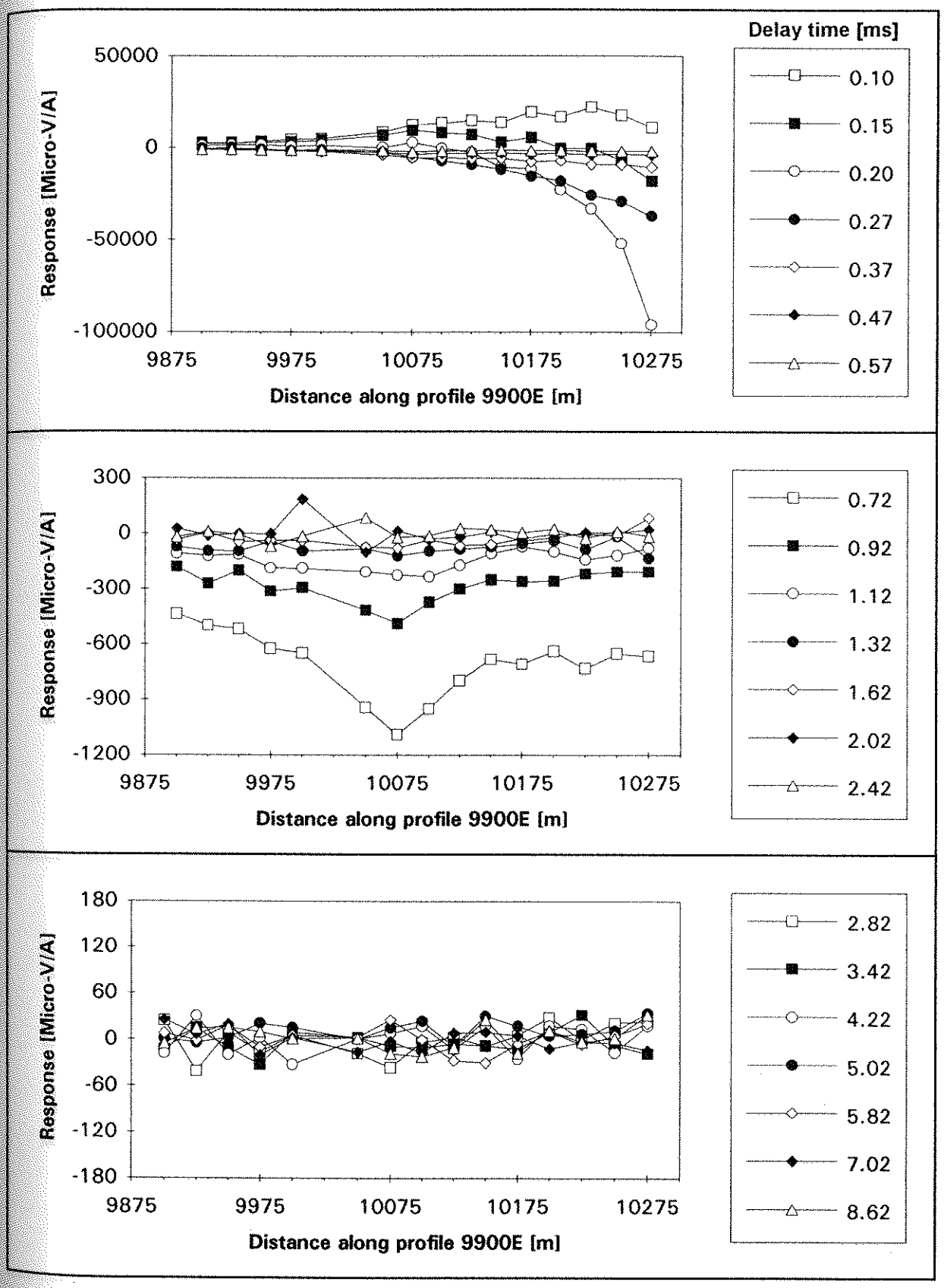

Figure 7.20 Fixed-loop geometry Y-component TEM response profile along profile 9900E obtained without applying an RNPF. These measurements were recorded with the computer-based noise system.

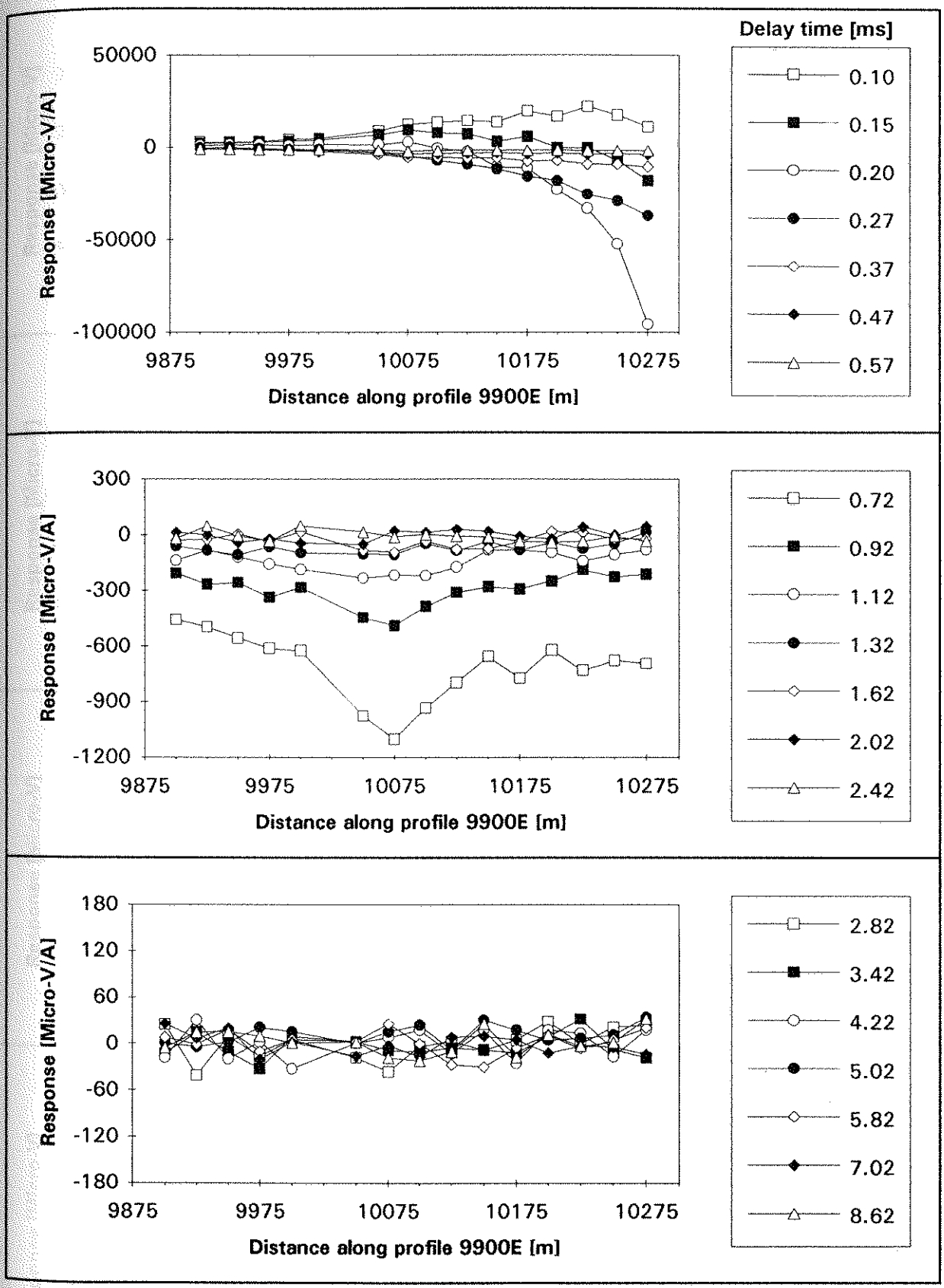

Figure 7.21 Fixed-loop geometry Y-component TEM response profile along profile 9900E obtained by applying an RNPF. These measurements were recorded with the computer-based noise system.

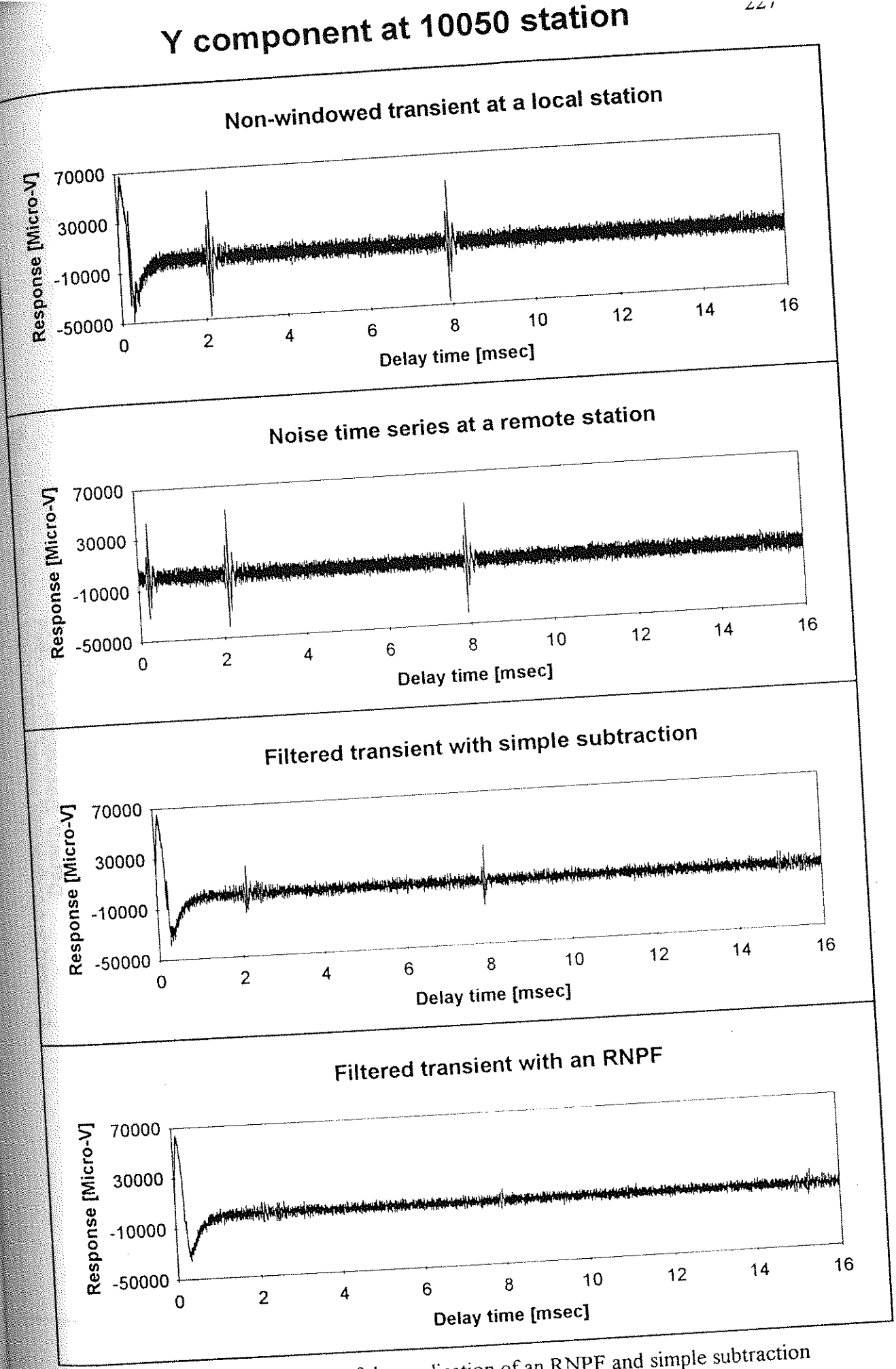

Figure 7.22 Comparison of the application of an RNPF and simple subtraction to the Y-component time series measured simultaneously at station 10050N and the remote station.

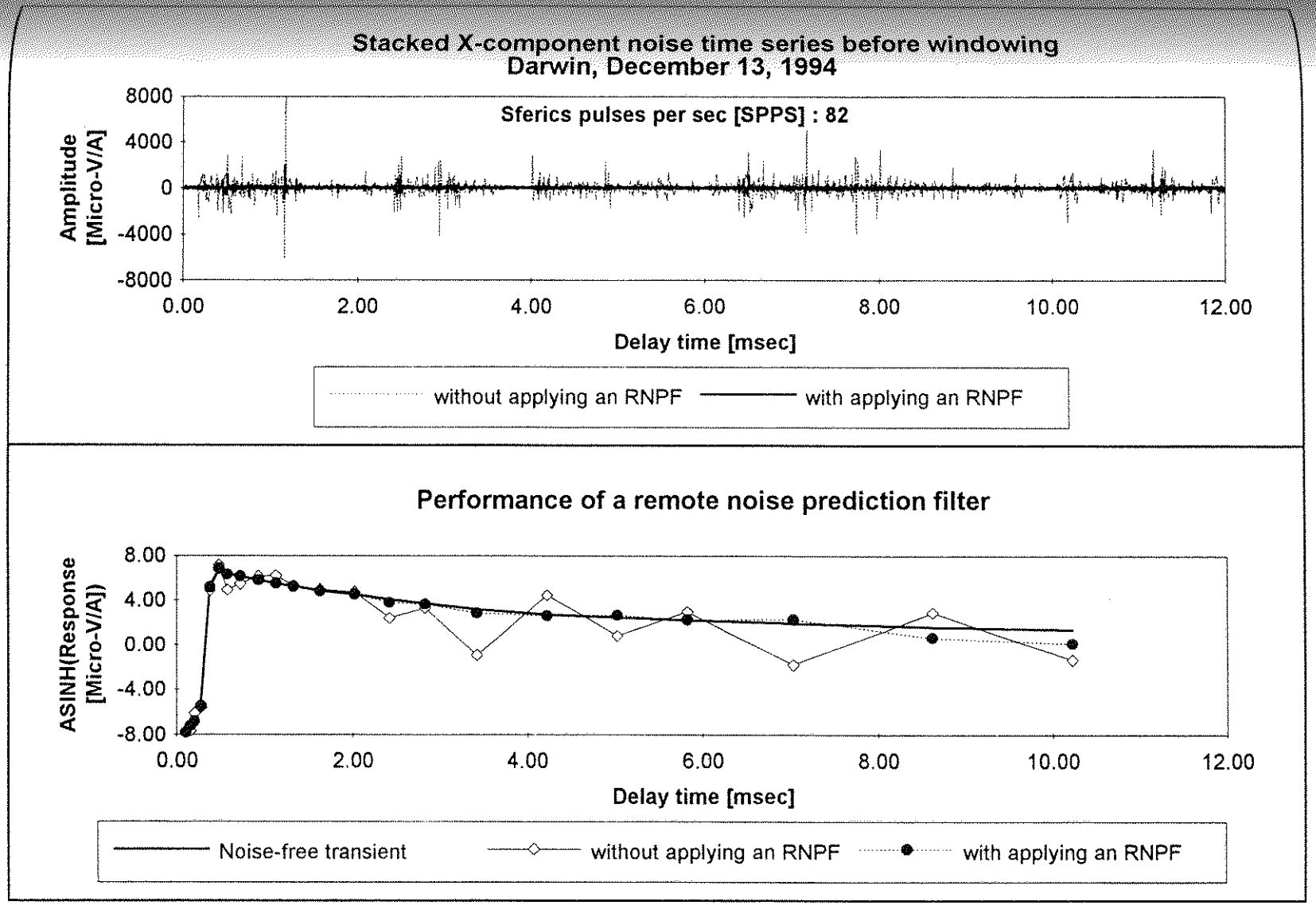

Figure 7.23 Example of the application of an RNPF to high sferics activity data measured in Darwin in December 1994. The local and remote time series were measured simultaneously with a separation of 1 km. The top diagram shows two 50-bipolar stacked time series obtained with an RNPF and simple subtraction. The bottom diagram shows the generated noise-free transient at station 9950N and two transients obtained when the two 50-bipolar stacked noise shown in the top diagram were windowed and added to the generated noise-free transient.

SIROTEM data collected at station 9950N with the fixed-loop geometry. The noise data before and after application of an RNPF shown at the top of Figure 7.23 were windowed according to the SIROTEM composite time scheme and added to the noise-free transient. The bottom diagram of Figure 7.23 shows the transient response before and after application of the RNPF. The filtered transient from an RNPF is very smooth at all delay times, while the simple stacked transient shows very poor S/N ratio even at the early delay times.

7.2.2.2 Vertical component

Figures 7.24 and 7.25 show a comparison of two X-component sferics measured with a receiver separation of 2 and 4 km, respectively, at the mineral prospect near Parkes. In both cases, compensation has been made for any time shift between the sferics pulses measured at the two stations. This time shift arises from any difference in the time of arrival of corresponding sferics pulses at the two receivers. This compensation introduces an inappropriate time shift into the background VLF noise, and the sferics waveform differences shown in both figures are considered to be caused mainly by the time shift introduced into the background EM noise (i.e., 44 kHz) rather than by a change in ground conductivity from one station to the other.

However, the vertical component sferics is more affected by ground conductivity changes. For example, Z-component sferics measured with receiver separations of 2 and 4 km are shown in Figures 7.26 and 7.27, respectively. Since the horizontal component is not affected very much by a conductivity change from the local to the remote station, the two Z-component sferics at each separation have been compensated for any time shift between them by using the time shift derived from the corresponding horizontal components measured at the same time. A subtraction of the Z-component measured at the local station from that measured at the remote station can produce larger sferics noise than the original sferics pulse (Figure 7.27).

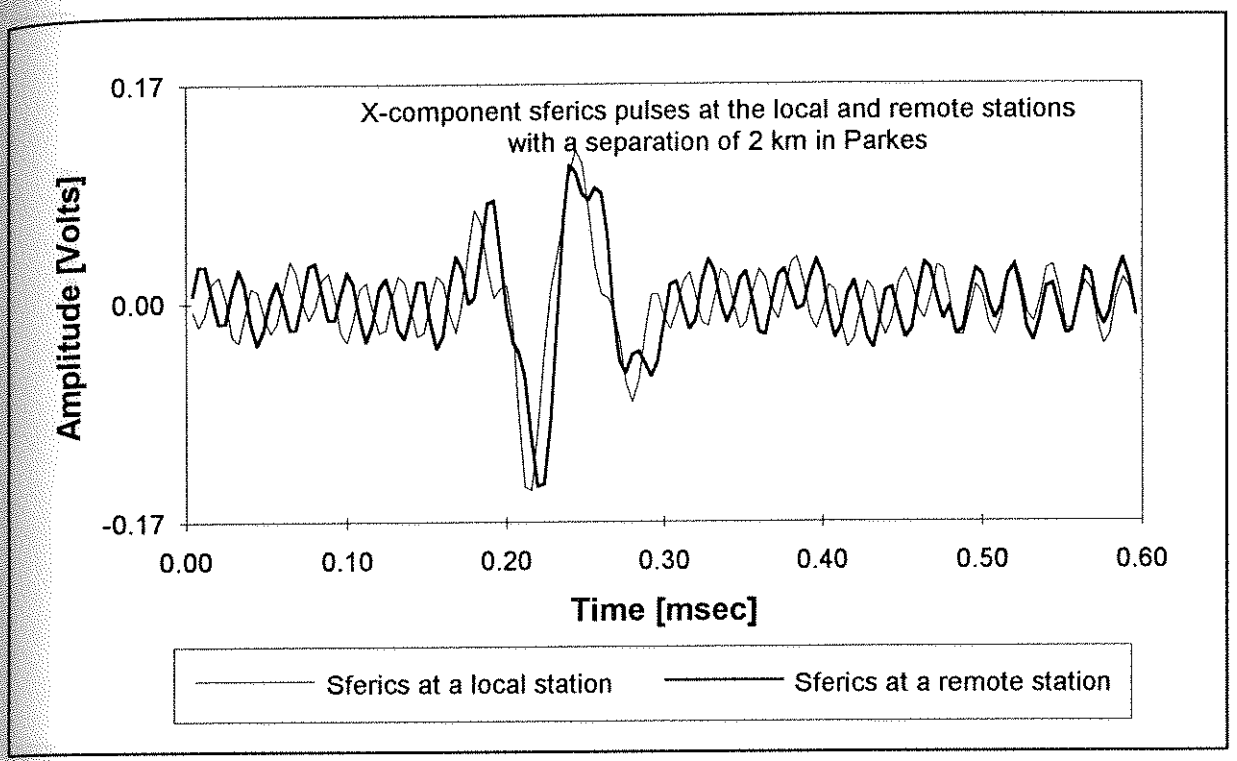

Figure 7.24 The X component of sferics measured simultaneously at the local and remote stations with a separation of 2 km near Parkes.

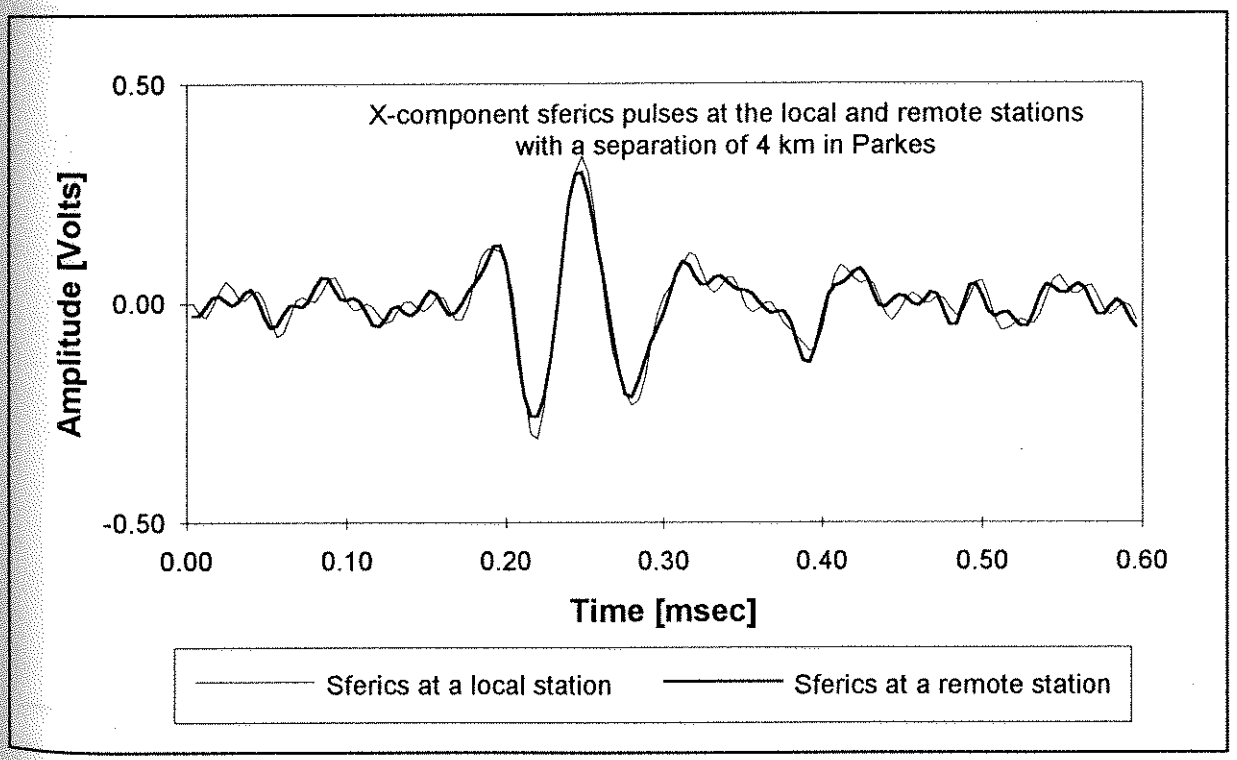

Figure 7.25 The X component of sferics measured simultaneously at the local and remote stations with a separation of 4 km near Parkes.

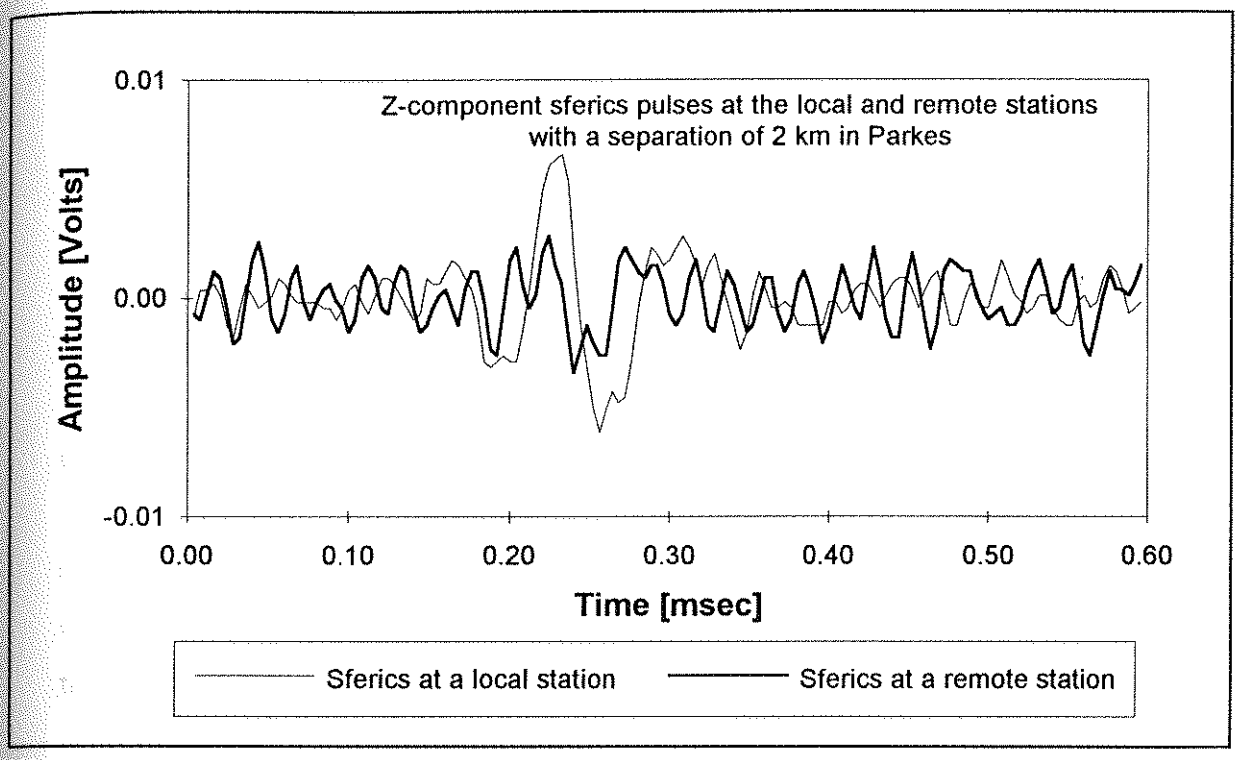

Figure 7.26 The Z component of sferics measured simultaneously at the local and remote stations with a separation of 2 km near Parkes.

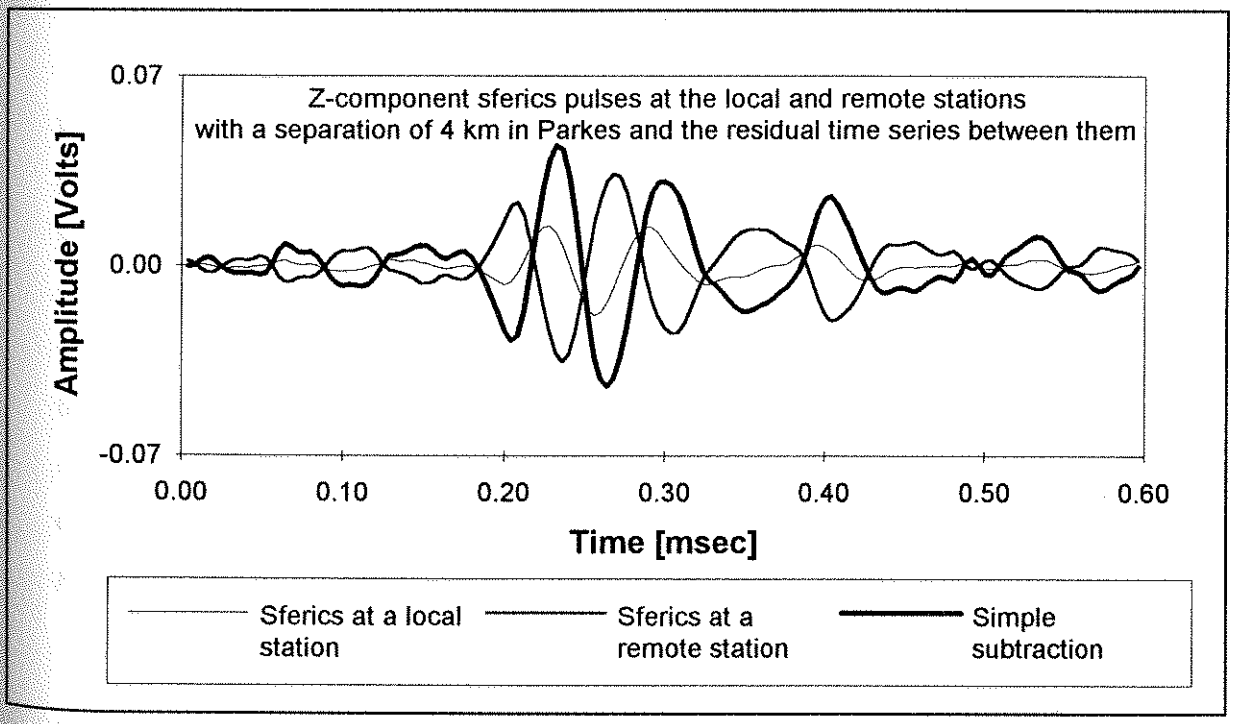

Figure 7.27 The Z component of sferics measured simultaneously at the local and remote stations with a separation of 4 km near Parkes and the residual time series obtained by subtracting between the remote from the local time series.

As mentioned in Section 5.6 of Chapter 5, the neural network configured to predict the local Z-component sferics using the remote Z-component does not produce as effective noise reduction as its application to the X or Y component. In order to improve the performance of the neural network based RNPF, an LNPF concept was introduced. For example, as shown in Figure 7.28, coherency spectra between the X and Z components at the local station and between the remote X and local Z components are very similar and show very strong correlation at a frequency range of 3 to 35 kHz, where power is contributed by sferics noise. Also, the coherency spectra between the Y and Z components at the local station and between the remote Y and local Z components show very similar patterns as the corresponding spectra between the X and Z components (Figure 7.28). Therefore, the network was reconfigured to predict the Z component using the remote X, Y, and Z components. This network is called the XYZ-RNPF.

Figure 7.29 shows the application of the XYZ-RNPF to reduction of sferics noise on the fixed-loop Z-component response measured at Parkes at station 9900N. The local and remote sferics pulses measured between delay times of 6 and 7 ms and two filtered time series obtained from the XYZ-RNPF and simple subtraction are plotted in Figure 7.30. *NRF* values of 0.6 and 2.0 were obtained from simple subtraction and the XYZ-RNPF, respectively, when the *NRF* value was calculated with the measured and filtered time series only between delay times of 6.0 and 7.0 ms shown in Figure 7.30. The transients shown in Figure 7.31 were obtained by applying the SIROTEM composite time windows to the transients shown in Figure 7.29. At delay times of 5.74 (window range of 5.24 to 6.24 ms) and 7.24 ms (window range of 6.24 to 8.24 ms), the fluctuations due to sferics noise are well removed by the XYZ-RNPF.

Figures 7.32 and 7.33 show the complete Z-component profiles before and after applying an XYZ-RNPF, respectively. Since the Z-component sferics is about ten times smaller than the horizontal component and the Z-component TEM responses are

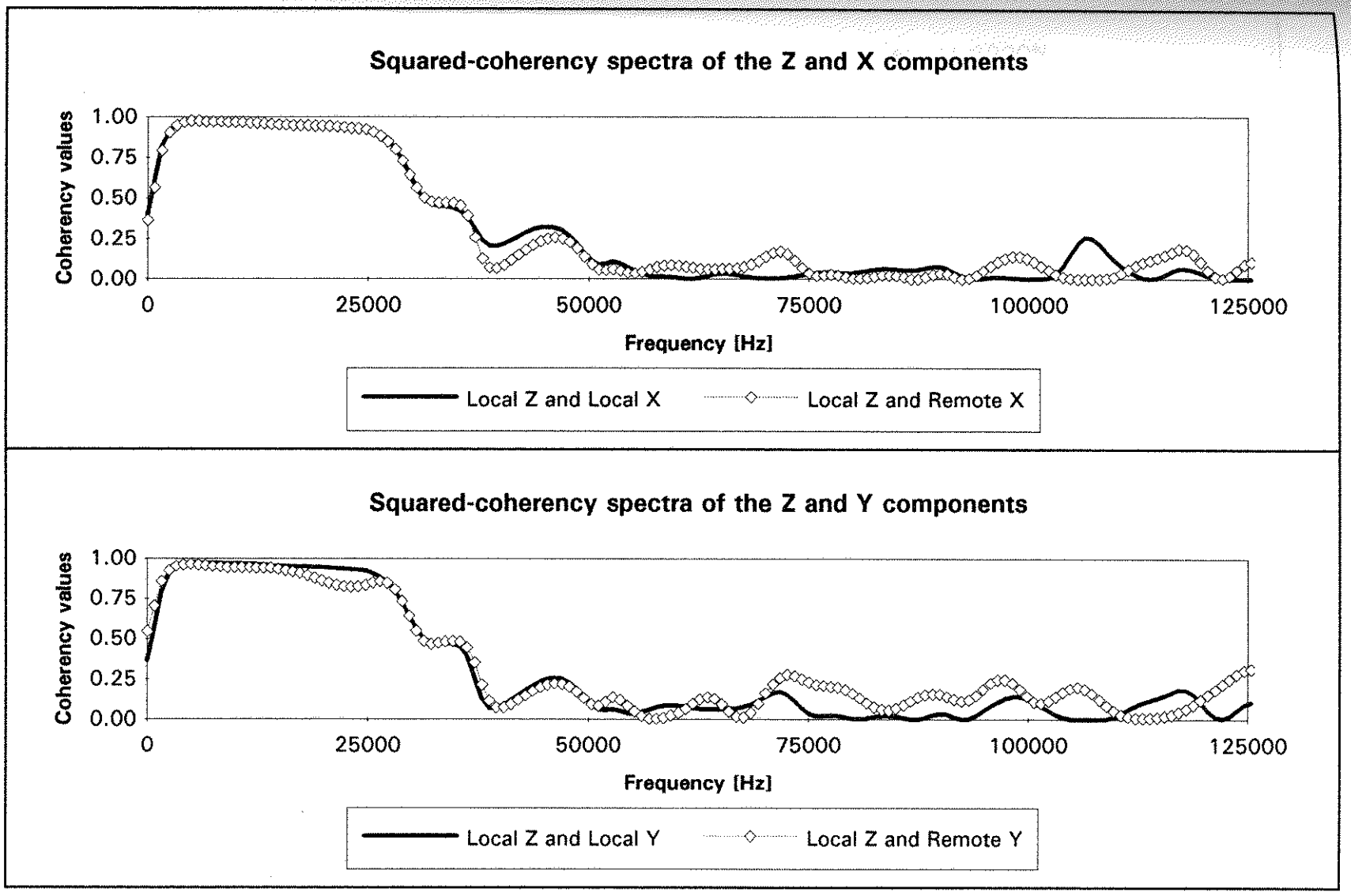

Figure 7.28 Example of the coherency spectra between the X and Z components measured at the local station and between the remote X and local Z components.

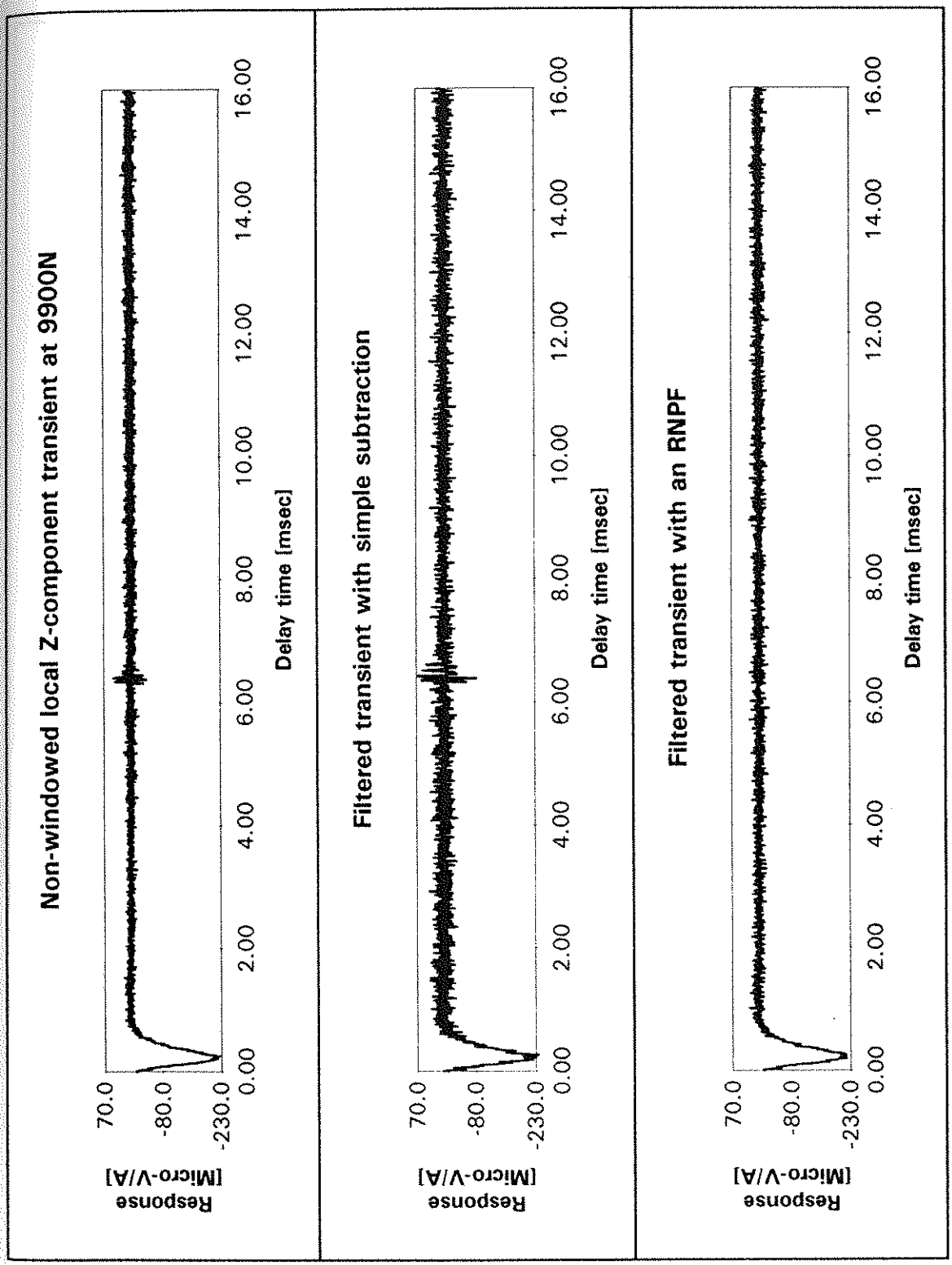

Figure 7.29 Comparison of the application of an RNPF and simple subtraction to the Z-component time series measured simultaneously at station 9900 N and the remote station.

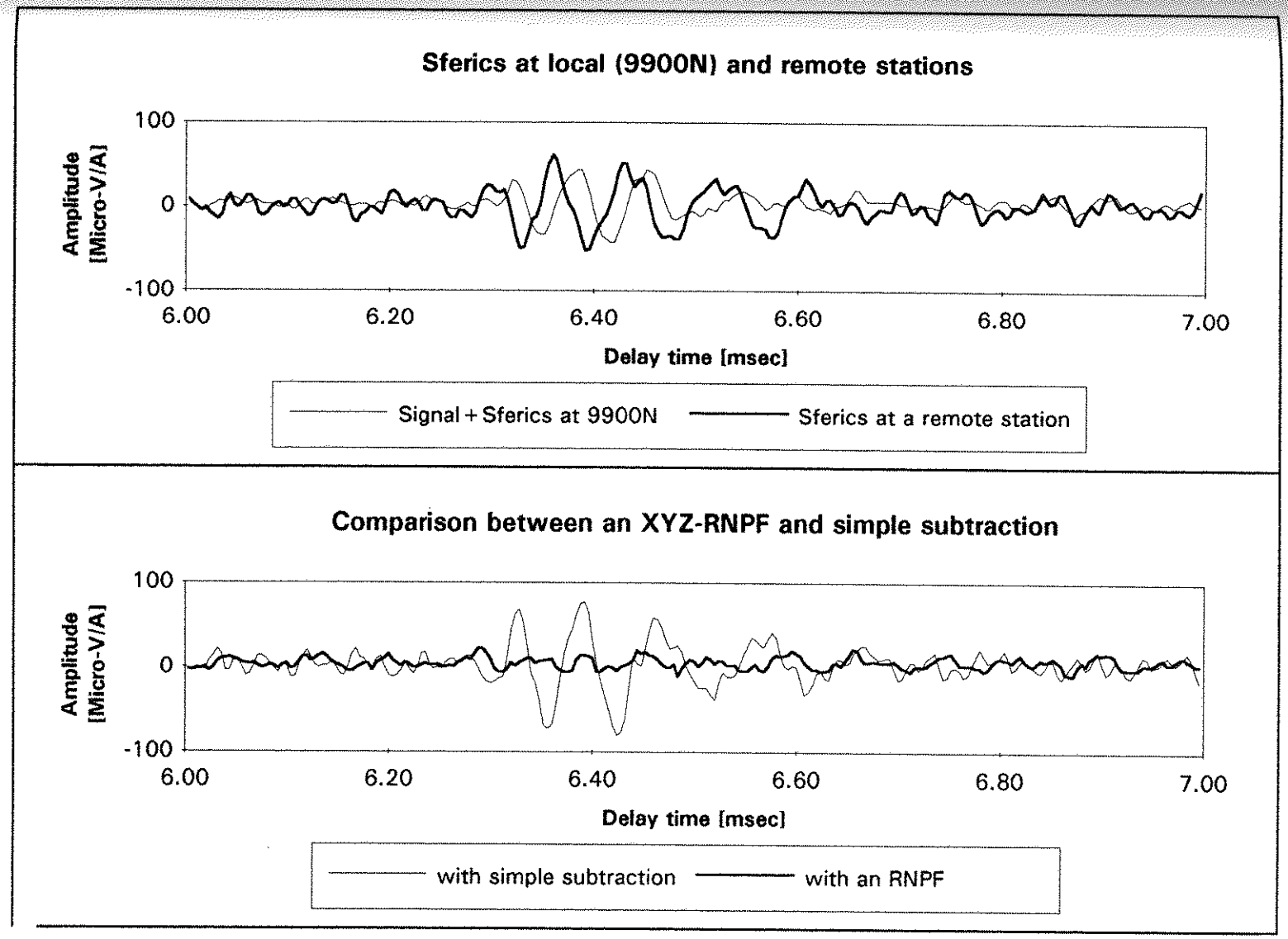

Figure 7.30 The local sferics pulse shown in Figure 7.29 and the corresponding remote sferics pulse between delay times of 6 and 7 ms, and two filtered time series obtained from an XYZ-RNPF and simple subtraction.

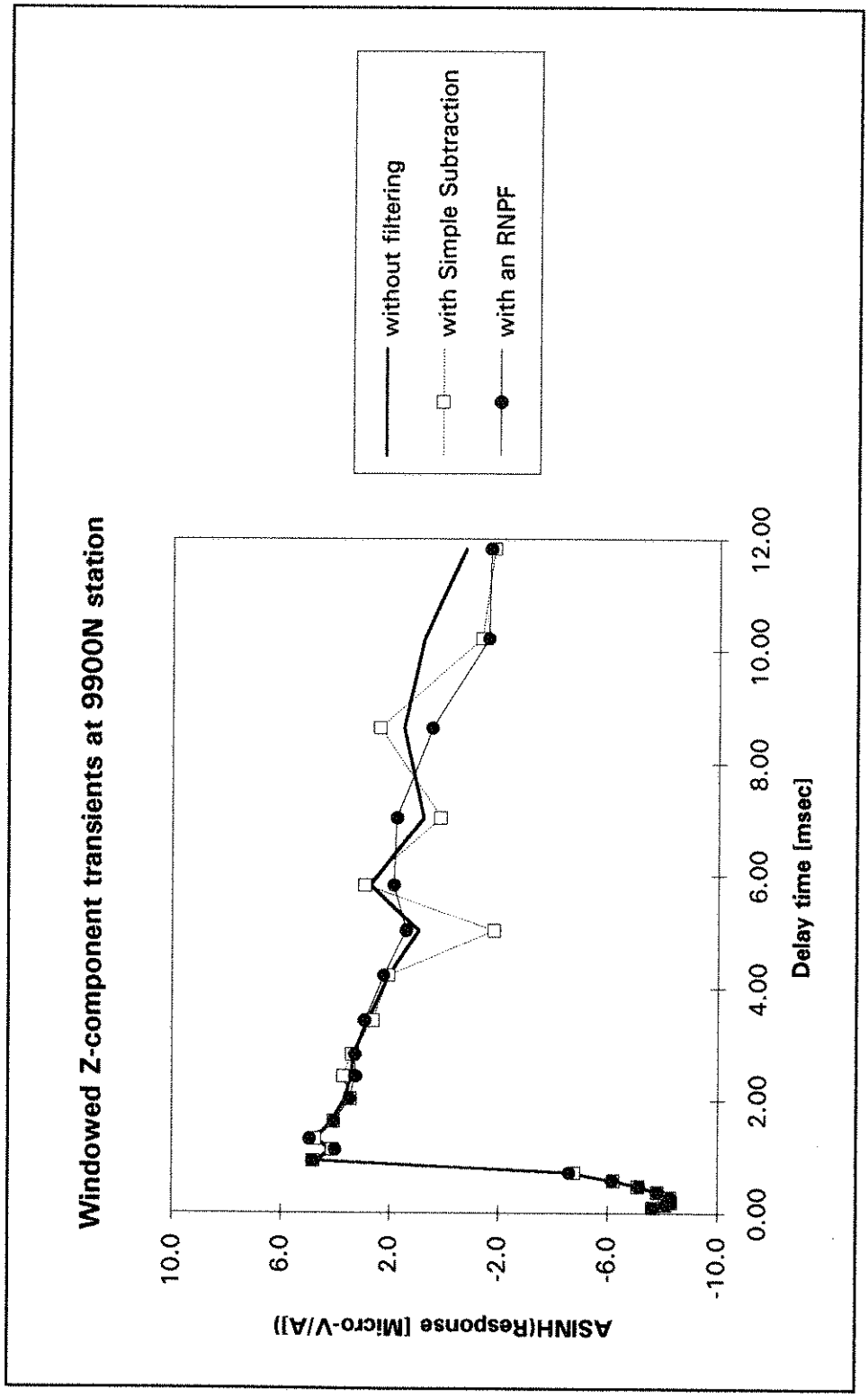

Figure 7.31 Three transients obtained when the SIROTEM composite time window scheme was applied to the non-windowed transients shown in Figure 7.29.

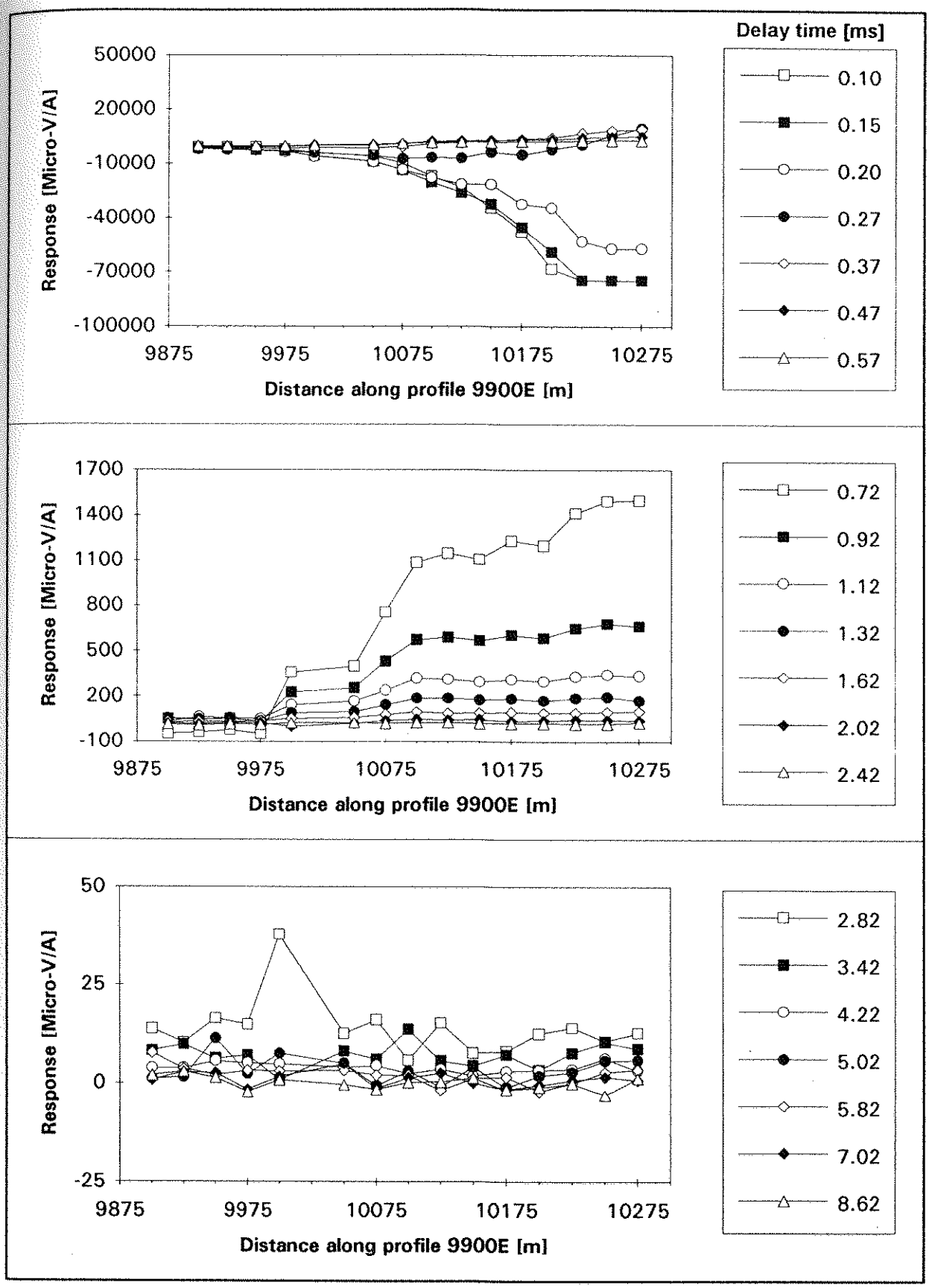

Figure 7.32 Fixed-loop geometry Z-component TEM response profile along profile 9900E obtained without applying an RNPF. These measurements were recorded with the computer-based noise system.

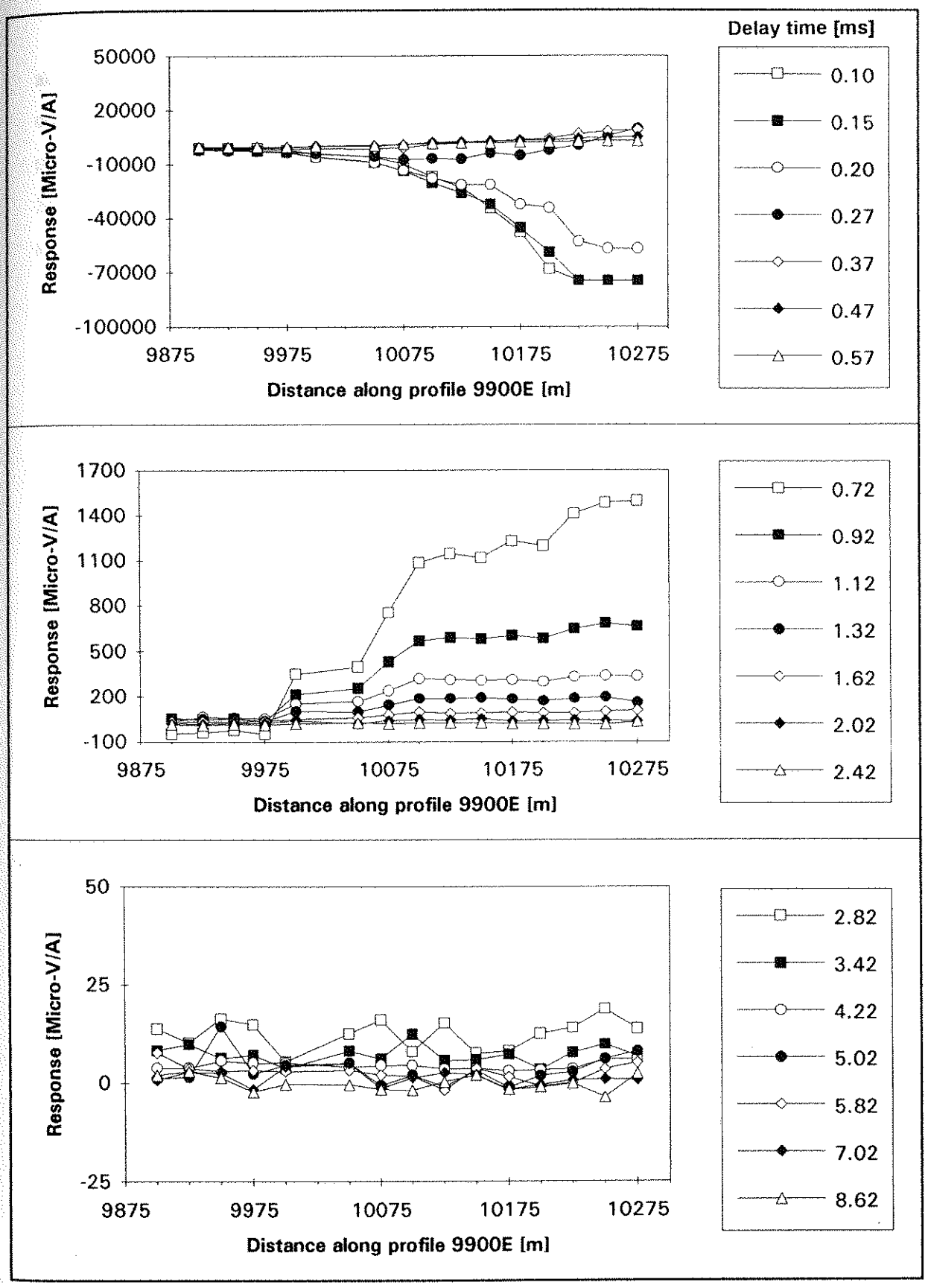

Figure 7.33 Fixed-loop geometry Z-component TEM response profile along profile 9900E obtained by applying an RNPF. These measurements were recorded with the computer-based noise system.

about 10 times larger than the X-component responses, most profiles are very smooth compared to the X-component profiles. Another example of the neural network performance is shown in Figure 7.34 where the response at station 10000N is plotted. Sferics noise around a delay time of 2.82 ms is suppressed by the XYZ-RNPF, while simple subtraction does not reduce the sferics noise at all.

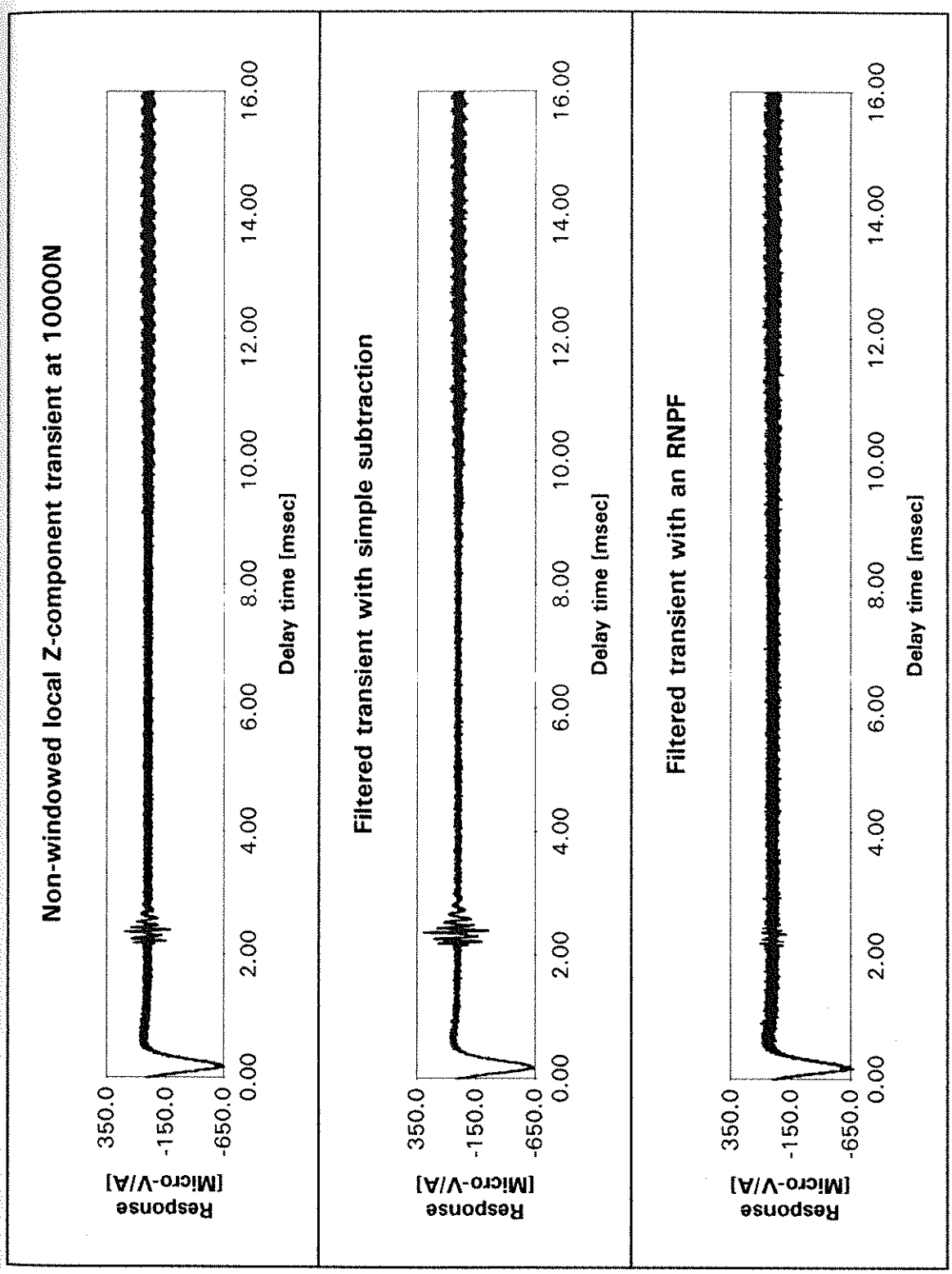

Figure 7.34 Comparison of the application of an RNPF and simple subtraction to the Z-component time series measured simultaneously at station 10000N and the remote station.

7.3 Conclusion

Analysis of SALTMAP data with 200 stacks at each station suggests that little or no sferics are present in the data compared with the SALTMAP system noise level. Even though the data were recorded in the late afternoon of 16:01:41 to 16:04:57 in summer, it is considered the measurements were made during a period of very low or no local sferics activity.

Neural network-based noise prediction filters have been applied to ground-based TEM data obtained in exploration conditions. TEM measurements with in-loop and fixed-loop geometries were made at a mineral prospect near Parkes in August, 1995. During these measurements, the sferics count rate was 6 pulses per sec, implying a very low sferics activity compared to the sferics count rate in Darwin in summer (e.g., a maximum of 123 pulses per sec).

In the application of a local noise prediction filter (LNPF) to in-loop TEM data, the neural network-based LNPF achieves very effective performance. Because of the lack of sferics in Parkes data, the performance of an LNPF was evaluated by adding sferics measured in Darwin in December 1994 to the in-loop TEM responses recorded at Parkes. The sferics count rate of the Darwin data used in this test is 76 pulses per sec, which is at least 12 times higher sferics activity than that of Parkes data. A noise reduction factor of 3.4 was obtained from the LNPF.

In the application of a remote noise prediction filter (RNPF) to the horizontal component TEM data obtained near Parkes with a fixed-loop geometry, neural networks were configured to predict the local horizontal component of sferics noise using the horizontal component of the corresponding sferics noise at a remote station. For both X- and Y- component sferics reduction, the network achieves good performance (i.e., *NRF* values of 4.0 and 4.8, respectively) in reducing the horizontal components of sferics pulses at the local station. Also, the performance of an RNPF

was evaluated with Darwin sferics data, which shows at least 13 times higher sferics activity than Parkes data. An *NRF* value of 4.7 was obtained when the RNPF was applied before stacking, while simple subtraction achieved the *NRF* of 3.4.

The vertical component of sferics shows a dispersive effect due to ground conductivity changes between the local and remote stations with both 2 and 4 km separations. In the application of an RNPF to the vertical component sferics, the network configured above does not produce effective noise reduction, since the dispersion effect makes it difficult for the neural network to recognise the amplitude changes and time shift between the two sferics pulses at the local and remote stations.

Squared-coherency spectra between the local vertical and remote horizontal components show very strong correlation in a frequency range where power is contributed by sferics (3 to 35 kHz). A neural network reconfigured to predict the local vertical component of sferics pulses using the remote three components of the corresponding pulses suppresses sferics noise down to the background noise level, while simple subtraction does not reduce sferics noise. For example, *NRF* values of 2.0 and 2.3 were obtained with such an RNPF at stations 9900 and 10000N, respectively, while an *NRF* value of 0.6 was obtained with a simple subtraction at both stations.